13

Microcalorimetric Approaches to Biopharmaceutical Development

Richard L. Remmele, Jr.

INTRODUCTION

A goal of biopharmaceutical development is to quickly move an investigative new drug into the clinic where it can be tested as a potential therapeutic to treat disease. To realize this goal, an enormous amount of effort must be carried out from conception in discovery to upstream, downstream, and formulation development stages. Much of this effort is guided by the generation of analytical data to help support optimization of yield, purification, and stability. Even with this strategy in place, there is room for better approaches to minimize any developmental bottlenecks. More rapid or "high-throughput" strategies and data-assimilation technologies are currently being used and evaluated at various stages of the process development assembly line. Within the past 20 years, mutagenic and recombinant technologies have shed light on structure–function relationships that have spawned from the protein engineering era. Given these strides, it is now possible to begin thinking about discovery biologics in terms of rational protein drug design.[1,2] As the science continues to advance, it would seem inevitable that one day accurate predictions about structure, function, and stability will greatly enhance therapeutic drug discovery, development, and approval. This also means that by simply understanding a disease, it could be possible to implement *de novo* design strategies to develop appropriate candidate biologics with the robust qualities of functionality and stability to cure or treat it. A necessary part of protein engineering would then involve building into the molecule the necessary conformational

attributes that make it efficacious, nonimmunogenic, and stable. Moreover, it is important to acquire and apply knowledge that has its roots firmly planted in the laws of thermodynamics and kinetics. Thermodynamic and kinetic properties of biologics as they pertain to mode of action (i.e., ligand–receptor binding, antagonist), structure, and overall stability will therefore continue to play an integral role in biopharmaceutical development strategies.

Among the many biophysical techniques that may be considered, microcalorimetry offers some clear advantages. It can directly measure enthalpic change and is useful for defining important thermodynamic parameters (i.e., thermostability, heat capacity, free energies, entropies, binding affinities) that can aid the discovery, upstream, downstream, and formulation development operations. As more knowledge about the physicochemical characteristics of a broad array of protein therapeutics is amassed, it should be possible to bioengineer a protein therapeutic with the right properties that make it efficacious, robust to the stresses of the process, and stable in the desired dosage form. This is the end result of biopharmaceutical development. If successful in the prediction of a well-characterized product, this approach could greatly reduce bottlenecks in the manufacturing sector.

This chapter will explore the relationship of thermodynamic and kinetic data as it pertains to characterizing the stability of various protein systems in the liquid state. Finally, from the wealth of information generated over the past few decades, it should be possible to assess the practical use of microcalorimetry for predicting stability. This technique used in combination with several other bioanalytical methods can serve as a powerful tool in the measurement of thermodynamic and kinetic phenomena.[3–9] Attention will be given to limitations of the technique rendered from different applications as well as to areas where it is advantageous. Ultimately, the practical utility of this technique will rest with those familiar with the art.

FUNDAMENTAL PARAMETERS OF MICROCALORIMETRIC MEASUREMENTS

There are several parameters that can be measured or determined using microcalorimetry that enable one to study the energetics of biomolecular processes at the molecular and cellular levels. Heat or enthalpic effects are intimately linked to biochemical processes that involve a change of state that can include a transconformational event often leading to enhanced instabilities.[10–15] Systems that undergo state changes will either liberate (exothermic reactions) or absorb (endothermic reactions) heat. Because the amount of heat involved in such reactions is often quite small (on the order of microcalories), highly sensitive instruments are needed to quantitatively measure protein reactions.[16] These instruments operate on the basis of measuring the microcalories of heat absorbed or liberated by a given process (i.e., protein unfolding, association, binding) as a function of the scanning rate against a suitable reference that contains the identical solution

environment without protein. The change of state accompanying the reaction, although sometimes characterized as "two-state" behavior, is really descriptive of an ensemble of microstates that predominantly populate two different states of the molecule.[17] This could take the form of a native and fully denatured state, or it could involve a transition from the native state to a partially folded intermediate state that depends on the conditions of the solution environment and the stresses involved (i.e., pH, temperature, chaotrope). This type of information can be important in describing the stability of a given biologic in a given environment (i.e., solution matrix). Other parameters that can be assessed using this technique include the free energy of unfolding, denaturation heat capacity, and entropy. Because all of these parameters are associated with changes of state described by an equilibrium process, they are all thermodynamic quantities.

The Melting Transition Temperature (T_m)

Consider a two-state system in which the protein exists predominantly in either its native or thermally unfolded state. The equilibrium describing such a system depends on temperature that in turn determines the population of the two states. At low temperatures the protein will largely exist in its native conformation. Although not always the case (i.e., α-lytic protease of bacterium *Lysobacter enzymogenes*), the native state is generally described as having relatively lower free energy than the unfolded or denatured state. A delicate balance exists between the forces that act to maintain the native form and those that would cause it to denature. Unfolding occurs as heat energy (enthalpy) loosens the protein structure by weakening the bonds and physical forces that maintain conformational integrity. The major destabilizing force is conformational entropy, and those that stabilize the native state are hydrogen bonding and the hydrophobic effect.[18,19] The thermally unfolded state is a denatured state. For sake of clarity, the term *denaturation*, used in this regard, will refer to "a process (or sequence of processes) in which the conformation of polypeptide chains within the molecule are changed from that typical of the native protein to a more disordered arrangement."[20] Hence, partially folded or intermediate states can be considered denatured states. During a typical heating experiment within the microcalorimeter, the denaturation transition is observed as an endothermic quantity arising from significant alterations in structure associated with unfolding. This process is identified as melting of the protein, and has an associated temperature, the T_m or melting temperature. This parameter is taken as the temperature at peak-maximum, where approximately half of the protein is denatured.[21,22] It is important as an integral parameter of the modified Gibbs–Helmholtz equation (defined in the following text) and also because it indicates thermostability.

An important consequence of thermostability is the attainable level of stability indicated by the T_m. For example, different solution environments can cause the T_m to shift.[23–27] A shift to higher temperatures by adding different excipients and/or changing the pH of the solution can be extremely helpful in

defining solution properties that are optimal for stabilization. The more easily unfolded or structurally perturbed (described by lowering T_m) from the native conformation, the more vulnerable the protein potentially becomes to instability. Protein unfolding can often augment a multiplicity of instabilities that include aggregation,[10–12,28,29] deamidation,[15] oxidation,[13] and proteolysis.[30] In these cases it is important to recognize that the prominence of the T_m to accurately describe stability is related to whether or not the degradation depends on unfolding. Therefore, the strategy in formulation development is always to impose a solution environment that prefers the native state in order to minimize the deleterious consequences associated with the instability of the product. By shifting the equilibrium in the direction of the native state, resulting in higher T_m, thermostability can be a useful parameter to define the solution variables that make it more difficult for the protein to unfold.[31,32]

An illustration of the unfolding for a multidomain protein is presented in Figure 13.1. It is the unfolding of IL-1 receptor (type I) that shows two predominant unfolding features (inlay) with T_m at 53.3°C and 66.7°C. After baseline correction, the T_m changes slightly to become 53.1° and 66.3°C, thus resulting in a small adjustment in the T_m of a few tenths of a degree. The inlay in Figure 13.1 also shows the reproducibility of two completely independent scans that are virtually superimposable. This is testimonial to the kind of precision attainable using this technique, given that it portrays complete alignment of the T_m in both scans.

Reversible vs. Nonreversible Systems

An inherent property of thermodynamic systems is an equilibrium between at least two states. In many cases the unfolding of a protein can be more complex than two states. Such an equilibrium can be verified by determining the reversibility of the process defining the two states. Using microcalorimetry, this may be evaluated simply by examining the enthalpy of two subsequent heating scans (given by the equation: % reversibility = $[\Delta H_2/\Delta H_1] \times 100$, where the subscript numbers designate the first and second scan results). Both the T_m and the enthalpies of unfolding should afford a significant measure of reversibility. The thermal reversibility of a number of protein systems has been described in the literature.[9,33–36] The thermodynamic significance of the calorimetric parameters requires evidence of thermal reversibility. Despite this need, can useful information about the energetics of a process be obtained from systems that exhibit nonreversible behavior?

To answer this question, information obtained from studies of irreversible systems needs to be examined. Irreversible protein processes may occur as a result of intermolecular interactions (i.e., aggregation, chemical modification, intermolecular cross-linking). Although an attempt is generally made to search for conditions that provide maximal reversibility, perhaps by altering the solution conditions (i.e., pH, salt content, lowering the protein concentration) that minimize contact and electrostatic interactions, many systems can still exhibit little or no reversibility. This would be the case for the core protein obtained by limited

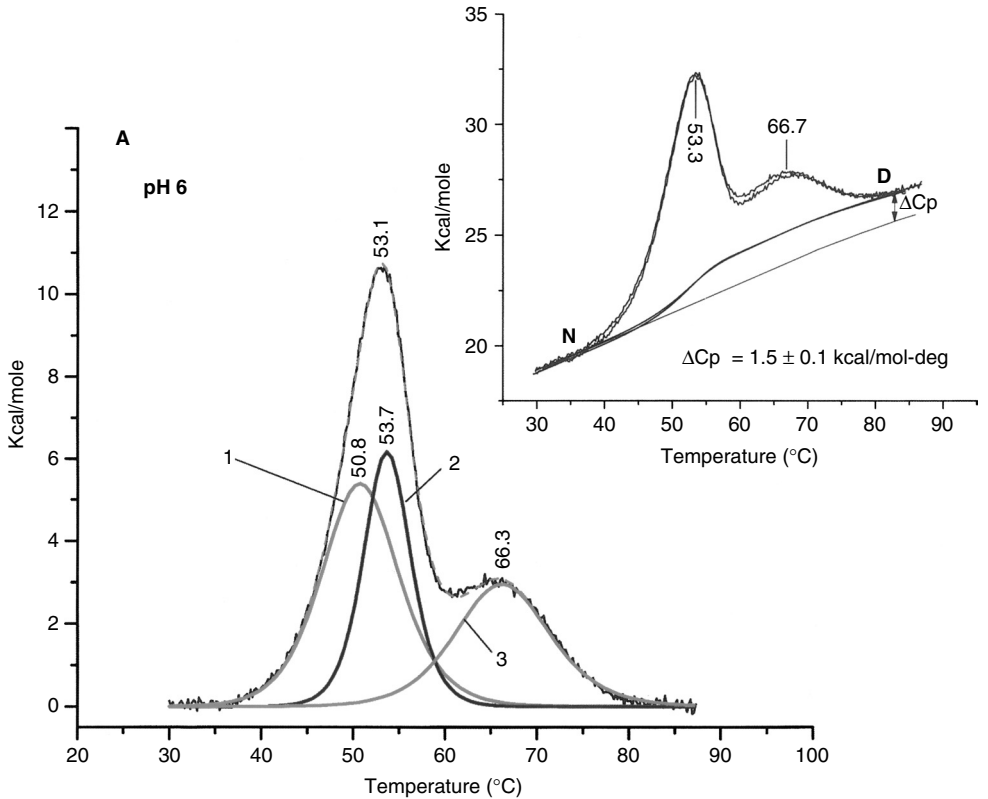

Figure 13.1 Microcalorimetry scans displaying T_m values for interleukin-1 receptor (IL-1R type I). The inlay displays the unfolding of IL-1R (I) showing the ΔCp measured as the baseline difference between the native (N) and denatured (D) states for two independent scans. Thermal unfolding of IL-1R (I) is composed of three cooperative unfolding transitions, labeled 1, 2, and 3.

proteolysis from the *lac* repressor of *E. coli*. It is tetrameric at ambient temperatures and irreversibly denatures during differential scanning calorimetry (DSC) heating experiments, yet it yields estimates of ΔHv (van't Hoff enthalpy) using three different methods (e.g., curve fitting of the endotherm, calculation of the van't Hoff enthalpy, slope of a van't Hoff plot) that were all found to be within reasonable agreement.[22] These results suggest that it is possible to apply equilibrium thermodynamics to irreversible processes. However, this evaluation still assumes that a reversible process is in operation. It is therefore preferable that reversibility be demonstrated in order for equilibrium thermodynamic parameters to be meaningful.

It is also possible to use microcalorimetry to obtain useful information about the kinetic processes of the instability (i.e., aggregation, proteolysis) when thermal irreversibility prevails. Scan rates will often distort the onset behavior of the melting transition that can necessarily impose a shift in the T_m, as discussed further in the following text. The scan rate dependence of the T_m may then be used to determine the activation energy of the instability, provided an Arrhenius kinetic model describes the behavior.

Heats of Reaction

During a calorimetric heating experiment, the quantity that is being measured is heat. Depending on the reaction, heat may be liberated or absorbed during the experiment. Unfolding of the protein during a heating experiment is necessarily an endothermic process. The endothermic quantity of heat for the unfolding process is referred to as the calorimetric heat of unfolding, ΔH_{cal} (also referred to as ΔH_m). It is obtained by integrating the area under the endothermic transition.[37] Another important endothermic parameter is the van't Hoff enthalpy (given by the equation $\Delta Hv = 4RT_m^2/\Delta T_{1/2}$, where R is the gas constant, and $\Delta T_{1/2}$ is expressed as the absolute transition temperature width at half-height).[38] It is important from the standpoint that if an unfolding event is two-state, the $\Delta H_{cal}/\Delta Hv$ ratio should be very close to 1. Hence, one can ascertain if a particular unfolding reaction is two-state or not. If this ratio is greater than 1, then more than two states must be significantly populated at equilibrium.[38,39] On the other hand, if this ratio should be less than 1, it is probable that the unfolding process involves intermolecular cooperativity.[40]

Exothermic transitions typically arise from protein–protein interactions that lead to precipitation.[28,41,42] These occurrences during heating experiments are good indications that the unfolding process involves aggregate formation. Circumstances underlying such behavior may lead to more complex unfolding patterns than can be described by a tri-state model.[43] For example, when aggregation is a competing reaction that depends upon the equilibrium that defines the unfolded state, there is a tendency for the reaction to conform to some aspect of nonreversibility. When such conditions exist, the irreversible step (or steps) are kinetically controlled and thus are not directly applicable to the treatment of equilibrium thermodynamics.[37,44]

Denaturation Heat Capacity

The heat capacity of thermal unfolding or denaturation (designated here as ΔCp) is positive because the denatured protein typically has a larger heat capacity than the native state. This parameter is believed to originate from the exposure of hydrophobic residues that are buried in the native state and subsequently become solvent-exposed in the unfolded state.[45] It can be measured in three ways. It can be determined as the heat capacity difference between the pre- and posttransitional baselines associated with the unfolding enthalpic envelope.[21] A representation of this behavior is described in the inlay of Figure 13.1. Note that the low (pretransition) temperature baseline (below the onset or incipient melting of the protein) does not coincide with the same at the posttransition temperatures. In fact, it is the difference in heat between these two regions (the pretransition associated with the native and the posttransition associated with the denatured states) that determines the heat capacity change between the two states. Alternatively, the ΔCp can be obtained from the slope of a linear plot of ΔH_m as a function of T_m, where T_m may be altered by changing the solution pH environment.[26,29] This latter method implies that the ΔCp is a constant parameter and is independent of temperature.[37] However, this issue will be discussed further in the following text because it has remained the subject of some debate. Finally, with the acquisition of greater sensitivity in microcalorimeter instrumentation, a new method has emerged that determines the heat capacity change from the slope of a linear plot of Cp as a function of the mass of protein in the calorimeter cell.[46] The denaturation heat capacity can vary in magnitude from 0.59 kcal/mol-°K (for Ovomucoid III) to 7.51 kcal/mol-°K (for phosphoglycerate kinase).[47]

Modified Gibbs–Helmholtz Equation

Protein stability has generally been defined in terms of the free energy change between the native and the unfolded states (ΔGu). This parameter of unfolding can be used to decipher stability of the native state across a wide temperature range.[48] The relation that incorporates all of the terms described above is the modified Gibbs–Helmholtz equation and is a function of temperature.

$$\Delta Gu(T) = \Delta H_m\,(1 - T/T_m) - \Delta Cp\,[(T_m - T) + T\ln\,(T/T_m)] \qquad (1)$$

Knowing the T_m (°K), ΔH_m (kcal/mol), ΔCp (kcal/mol-°K) permits calculation of the free energy change (kcal/mol) for the unfolding reaction at any temperature. This equation assumes a two-state mechanism in which the predominant forms are represented by the folded (native) and unfolded (denatured) states. Free energies of protein unfolding typically range from as little as 5 kcal/mol to 25 kcal/mol (a small energy threshold to overcome). It follows that proteins are essentially vulnerable to unfolding. However, the degree and extent of unfolding may not involve complete conversion to a random coil state. For example, it is known that denatured proteins retain a significant portion of native structure suggesting that, in some cases, partial unfolding is all that is required to form

aggregated products.[49–51] Equation 1 describes a parabolic function. At the temperature where $T = T_m$, $\Delta Gu = 0$. Given the fact that the function describes a parabola, there must not only be a T_m where $\Delta Gu = 0$ at elevated temperatures, but the equation predicts that the same is true at low temperatures (subzero in most cases) as well. The temperature where $\Delta Gu = 0$ at low temperatures is defined as cold denaturation.[21] Questions can arise about the validity of this equation if ΔCp is not constant over the temperature range considered. Evidence gathered would suggest that it is essentially independent of temperature within a finite range extending from approximately 20 to 80°C.[21] When considering temperatures beyond this range, in some cases it might be possible to check the accuracy of ΔCp over a broader temperature range by considering the accuracy of Equation 1 to predict cold denaturation.

Entropy

During a thermal heating experiment, the entropy (ΔS) of the protein logically should increase. If ΔGu can be determined by Equation 1, it follows then that ΔS may be determined from the expression $\Delta Gu = \Delta H_m - T\Delta S$. As the thermal energy of the system increases, the tendency of the protein to approach a state that is more structurally disordered is likewise expected. In fact, it has been shown for metmyoglobin (approximately two-state) that the enthalpy and entropy changes associated with Equation 1 increase with the temperature.[52] Knowing that ΔGu is essentially the work required to disrupt the structure of a folded protein, the temperature at which maximal stability is achieved (described by Equation 1) should coincide with the condition where the native and denatured states do not differ in their entropy values.[48] Entropy from the formation of a complex (i.e., protein–protein interactions) relative to the free molecule in solution is largely driven by hydration effects that involve polar and nonpolar groups. The nonpolar or hydrophobic groups will tend to order water molecules into networks of clathrate-like structure.[19] The apparent cost of this structure is a reduction in the entropy of the solvent. When such groups are removed from the aqueous environment as a result of protein binding (i.e., aggregation, receptor–ligand), there is a significant reduction of hydrophobic surface accessible to the water environment. This will lead to a large overall entropy change that is often positive.[53] This favorable change can be offset by a reduction in side-chain mobility as a consequence of binding that translates into an unfavorable contribution to the entropy gained by the solvent.

LIQUID FORMULATION DEVELOPMENT STRATEGIES

There are two primary questions that a formulator will often ask regarding a biopharmaceutical. First and foremost, what excipients (inactive ingredients like chemical stabilizers, buffers, and toxicifiers) and solution conditions (i.e., pH, temperature) offer the greatest stabilization? Second, how long will the chosen

candidate formulations remain stable? The first question addresses rank-order assessment of formulation composition based upon thermodynamic and chemical stability. If there were a way to predict the outcome of massive screening efforts that were designed to determine the optimal formulation candidates, this would prove to be a valuable step toward reducing time and cost that would otherwise be spent serendipitously trying to reach that goal. The second question deals with the kinetic processes associated with the degradation of the biologic. Typical projections for liquid biopharmaceuticals to remain stable usually target a 2-year duration. Microcalorimetry can be used to aid in the screening of excipients that stabilize the native state. This technique is well suited as already established (e.g., sensitivity to solution environment, protein-unfolding properties) to assess how different solution environments perturb protein unfolding. The primary objective in most cases is to maintain the native structure or conformation of the molecule in the desired dosage form.

pH Profiles

The first step in ascertaining the appropriate solution environment to store and stabilize a given biologic is to identify the pH conditions where it remains conformationally stable. This can be approached by examining the behavior of the T_m as a function of pH. This has been a successful strategy for the development of formulations for M-CSF and CD40L.[14,32] In these two particular cases, the T_m optimum correlated with the pH conditions in which aggregation was minimized. Figure 13.2 illustrates the pH profiles of several protein biologics manufactured at Immunex Corporation. Interestingly, preformulation conditions generally align with regions where T_m attains its highest levels. In the case of IL-1R (type II), optimal pH corresponded with the region of the highest T_m and low susceptibility to breakdown or aggregation instabilities. Once the optimal pH region is determined, appropriate buffers should then be chosen for the preparation of candidate formulations.

Here it is important to point out that buffers should be considered that exhibit little change with temperature because such dependence is proportional to the enthalpy of ionization of the buffering agent.[52] Alternatively, in order to minimize ionization effects and environmental changes during a given heating experiment, polybuffer systems have been used for pH profiling studies.[32] The polybuffer system used in the pH profiles shown in Figure 13.2 consisted of 50 m*M* sodium citrate, 20 m*M* NaCl, 20 m*M* phosphate, 17 m*M* L-arginine, 40 m*M* L-glycine, 25 m*M* HEPPS, and 20 m*M* HEPES. When all the ingredients are mixed together, the pH of the mixture is nearly neutral. One can simply add acid or base to adjust the pH from neutrality to the desired condition. Use of this polybuffer system was intended to normalize the influence of the buffering components and minimize the enthalpy of ionization. All of the buffering agents chosen minimize the pH dependence on temperature and permit adequate buffer capacity across a broad pH range extending from pH 3 to 11.

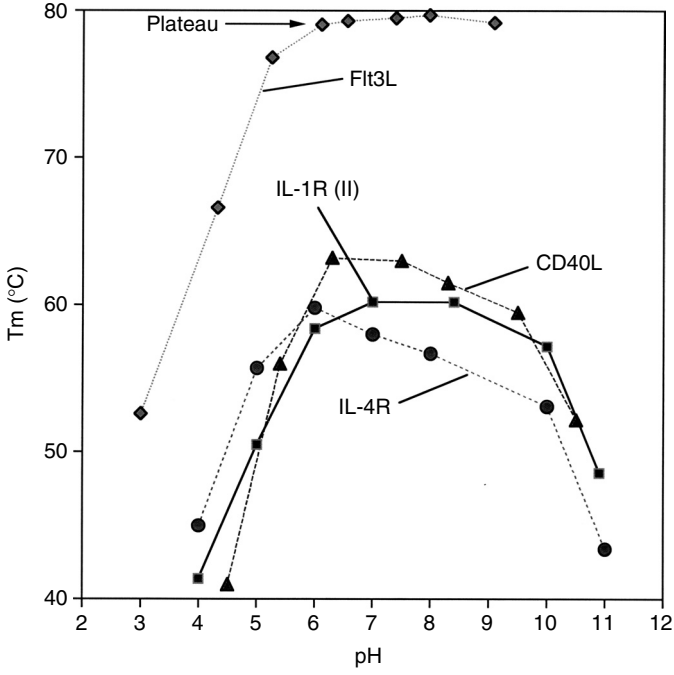

Figure 13.2 The pH profiles of several protein therapeutics. The data illustrate the behavior of T_m as a consequence of change in pH conditions. At the point where T_m essentially achieves a maximum across a broad pH range, a plateau is observed (as indicated for Flt3L). Note that these studies were conducted in the same polybuffer previously described.[54]

Thermal Reversibility

The second step toward defining stable conditions for the biologic is to evaluate (if possible) the thermal reversibility within the region of optimal pH. This was a successful approach in the development of a stable formulation for Flt3L.[54] In this case the solution conditions that best characterized minimal aggregation were found to occur where the thermal reversibility was greatest within the region of the T_m plateau (Figure 13.2). Even in the case of systems that are not thermally reversible (e.g., CD40L), pH profiling can still be advantageous in identifying the best conditions where stabilization is optimally achieved.[14] This is clearly illustrated in Figure 13.3, where the pH profile of the T_m behavior mirrors the tendency of the CD40L molecule to aggregate. The optimal pH region of the T_m profile matches the optimal pH region obtained from accelerated stability studies conducted at 37°C over 7 d.

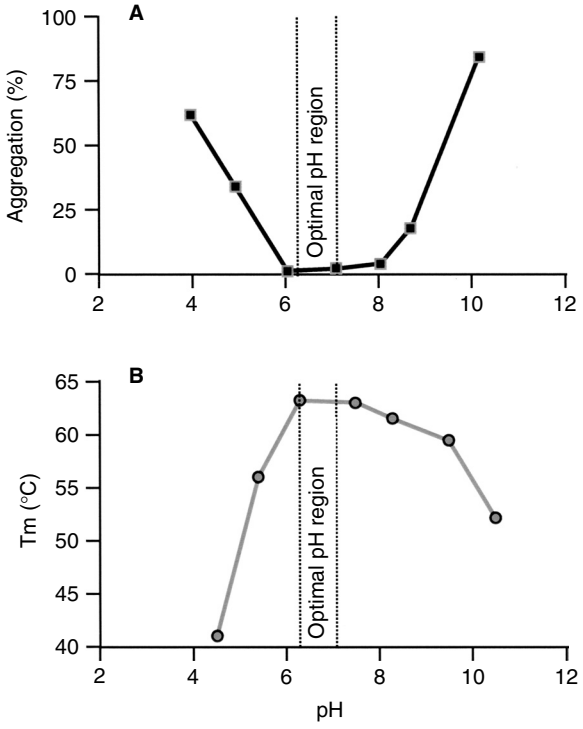

Figure 13.3 Stability behavior of CD40 ligand (coiled-coil CD40L trimer), showing the aggregation response obtained from accelerated studies (7 d at 37°C) as a percentage determined from size exclusion chromatography (A), and the T_m response (measured by microcalorimetry) as a function of pH (B). The bracketed vertical dashed lines represent the optimal pH region in which aggregation was minimized, corresponding to the same region in which T_m was maximized. Optimal pH conditions may be attained between pH 6 and 7.5. (Permission to use the figure granted by BioPharm.)

Excipient Screening

Once optimal pH conditions are determined and thermal reversibility is evaluated, manipulation of the solution conditions by screening stabilizing excipients (i.e., salt, stabilizers, other inactive ingredients) that further augment T_m and/or reversibility can be valuable. This was true for IL-1R (type I), where among 23 different excipient conditions, NaCl was shown to increase T_m to its highest attainable levels.[31] Additionally, the role of excipients on thermal reversibility is of some benefit for the stabilization of recombinant human megakaryocyte growth and development factor.[55] In another study concerning the stabilization of recombinant

human keratinocyte growth factor where a variety of osmolytes and salts were screened, NaCl, sodium phosphate, ammonium sulfate, and sodium citrate were highly effective in increasing both the T_m and storage stability.[56] Osmolytes and certain salts behave as protein stabilizers by being preferentially excluded from the vicinity of protein molecules, thus making the denatured state more thermodynamically unfavorable than the native state.[56–58] These excipients essentially drive the equilibrium in the direction of the native conformation and exhibit high melting transition temperatures.[56] The choice of additives (excipients) used to stabilize a biologic also depends on the properties of the protein (discussed in the following text).

The microcalorimetric technique is generally not well suited for high-throughput testing. However, using the information provided by the pH profile and a basic understanding of the kinetics involved with the instability (i.e., aggregation, breakdown), it should be possible (in some circumstances) to design appropriate accelerated studies to obtain the same answers over a broad array of screening conditions and over a shorter period of time. This is an alternative approach that has been used successfully to abridge this shortcoming. Once the accelerated studies reveal some selection of excipient conditions that improve stability, a check on these conditions can be evaluated in the microcalorimeter to confirm the effects on thermostability.

Use of Preservatives

At this point, if the formulated dosage form is to be a multidose presentation, preservatives will be necessary. Preservatives protect the product from microbial contamination during reentrance into the vial. A choice of several preservatives might be considered, such as phenol, benzyl alcohol, and metacresol. All can have a destabilizing effect on the protein as shown for IL-1R (type I).[31] Protein unfolding as a function of preservative concentration generally shifts the T_m to lower temperature accompanied by band broadening.[14] This behavior is presented in Figure 13.4, showing the effects of benzyl alcohol concentration on the T_m of a protein. While broadening of the transition envelope with decreasing T_m has been regarded as an indication of a large positive ΔCp for protein unfolding, penetration of the preservative into folded regions of the protein, facilitating an overall loosening of the folded structure, could also be a contributing factor.

The unfolding behavior of multidomain proteins in the presence of preservatives has also been evaluated. For example, IL-1R (type I) has three domains that correspond to three unfolding transitions as measured by microcalorimetry and depicted in Figure 13.1.[31] All three transitions exhibit some shift to lower T_m in the presence of the three preservatives tested (i.e., 0.065% phenol, 0.1% metacresol, and 0.9% benzyl alcohol), in comparison to a control containing no preservative. Such a destabilization could have consequences for the shelf-life of the product. Another example of the impact of preservatives on a multidomain protein is illustrated in Figure 13.5. The protein is fused to a single IgG_1 Fc. The

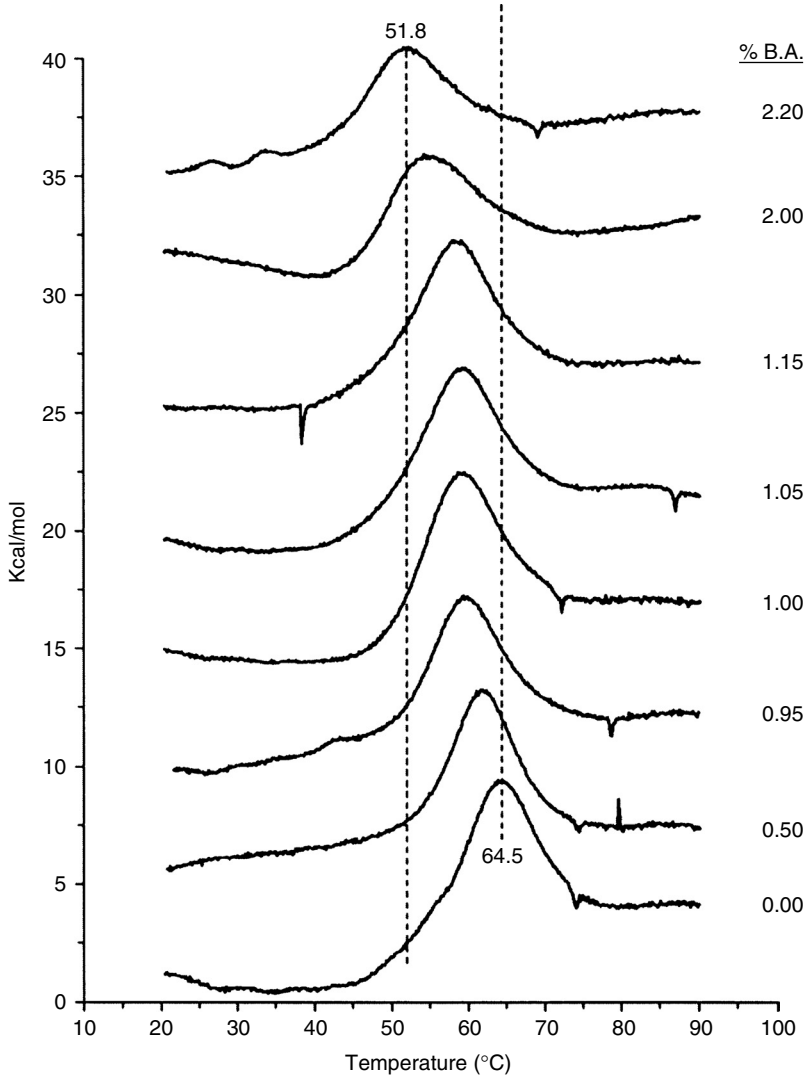

Figure 13.4 Perturbation of the melting transition temperature of a single domain protein as a function of benzyl alcohol content (described as % B.A.). The liquid protein formulation consists of 10 m*M* Tris, 4% mannitol, and 1% sucrose, pH 7.4. (Permission to use the figure granted by BioPharm.)

data show that 0.9% benzyl alcohol (dashed scan) destabilizes the two upper transitions by shifting them several degrees to a lower temperature. In contrast to the effect of the benzyl alcohol, 0.1% phenol had very little impact on the

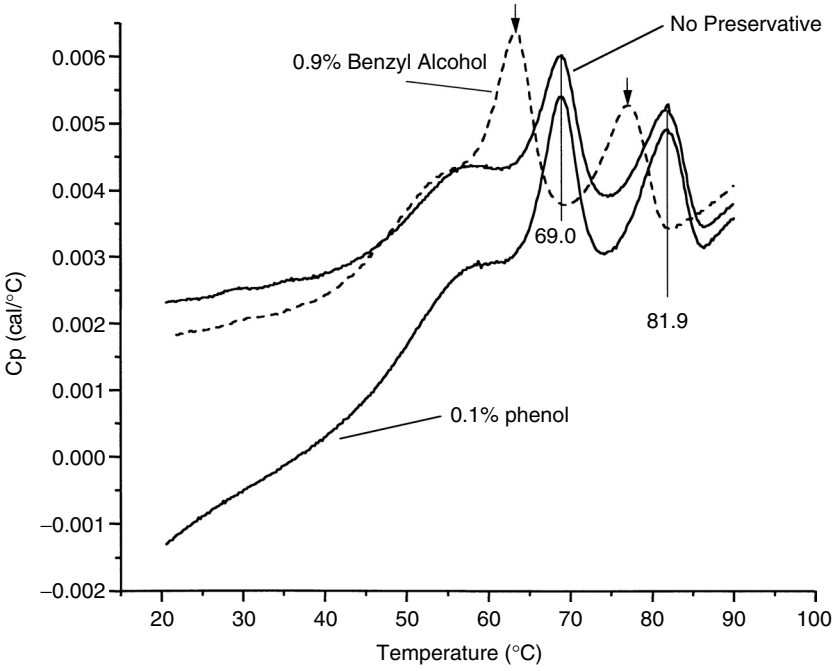

Figure 13.5 Microcalorimetry thermograms (not concentration normalized) showing the destabilizing influence of 0.9% benzyl alcohol (dashed trace) on two high-temperature transitions associated with the Fc domains of an IgG_1Fc fusion protein. Note that 0.1% phenol exhibits very little influence on the unfolding behavior of the protein in comparison to the control (not containing preservative).

unfolding behavior of the protein. Additionally, there may be a need to increase the amount of preservative, depending upon the outcome of preservative efficacy tests. If this is the case, it might be worthwhile to plot the change in T_m as a function of preservative content.[14] A plot of this kind for the benzyl alcohol data shown in Figure 13.4 is presented in Figure 13.6 and may be used to determine the type and amount of preservative necessary, while maintaining appropriate stability. The slope of such a plot indicates the destabilizing force a given preservative can exert (dT_m/dPv, where Pv represents the concentration of the preservative as a percent or as a mole ratio). If, for example, another preservative is evaluated that produces a smaller negative slope (described by the dashed line in Figure 13.6, denoted A) than that described by benzyl alcohol, it would exert less of a destabilizing effect on the protein, and a higher concentration could be used to achieve the desired preservative efficacy. The converse would be true for the situation described by the dashed line denoted B in Figure 13.6.

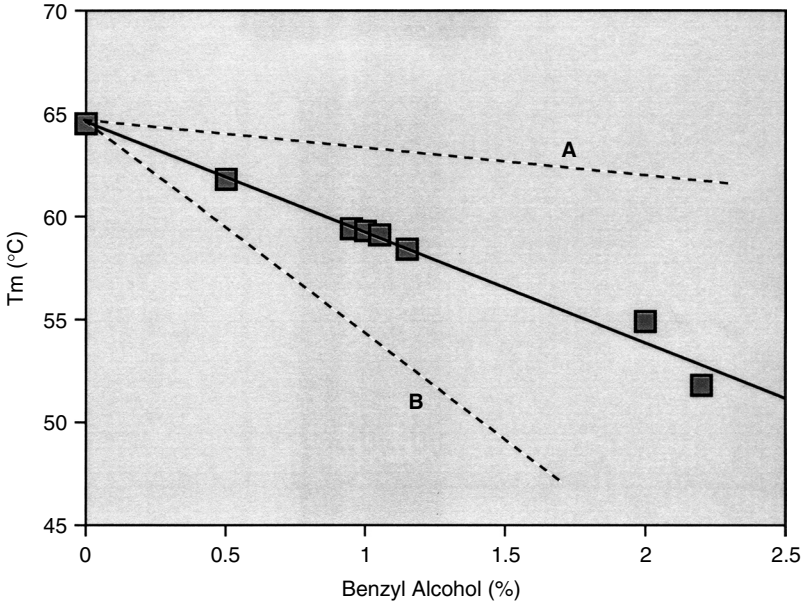

Figure 13.6 The relationship between T_m (°C) and benzyl alcohol content (obtained from the data in Figure 13.4) expressed as a percentage (w/w). Note that the relationship can be fitted to a line having a slope that describes the destabilizing force of the preservative. The dashed line designated as "A" illustrates a preservative force that is less destabilizing in contrast to the dashed line designated as "B" that is more destabilizing than benzyl alcohol.

It is also important to point out that stabilization against preservative effects may be augmented with appropriate excipient ingredients. This was the case for recombinant human interferon-γ (rhIFN-γ), where the interaction with benzyl alcohol was formulation dependent.[59] This study concluded that a stable preservative multidose liquid formulation could be achieved by minimizing the preservative concentration and using an acetate buffer at pH 5 (thermally stable condition). These results at least support the strategy described above, given that optimal pH conditions coupled with excipient screening (e.g., buffer, ionic strength) and benzyl alcohol concentration permitted a stable formulation to be derived.

Accelerated Stability

Finally, the last step in the preformulation development process is to test the candidate formulations that exhibited the greatest overall stability, using microcalorimetry. The true test of the procedure summarized in Figure 13.7 is to

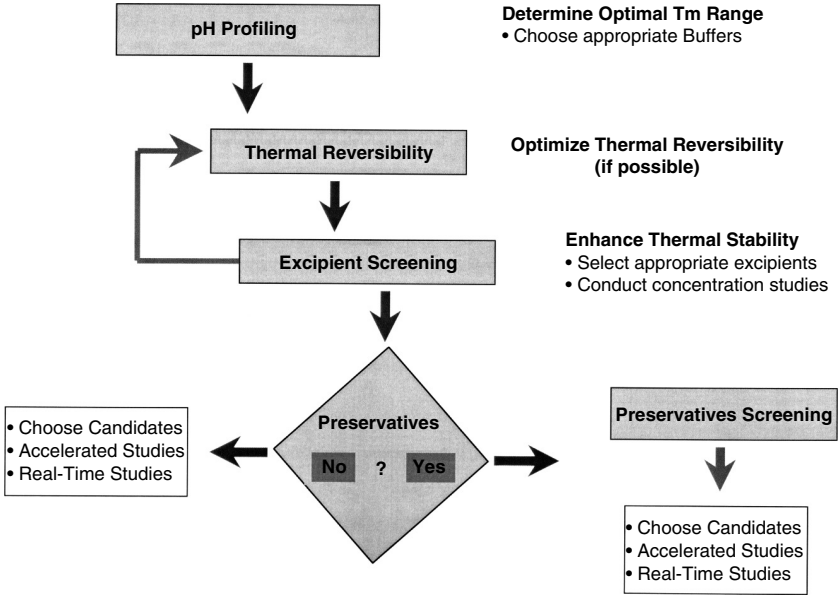

Figure 13.7 A formulation strategy using microcalorimetry aimed at deriving stable liquid candidates.

evaluate the predictive outcome by carrying out accelerated stability studies. In the case of IL-1R (type I), using the T_m as a measure of the influence of preservatives to destabilize the three transitions in this molecule, the predicted stability would have followed control (no preservatives) > 0.065% phenol > 0.1% *m*-cresol > 0.9% benzyl alcohol.[31] Accelerated studies were conducted at the physiological temperature of 37°C for a period of 60 d and yielded the results shown in Table 13.1. Clearly, the quantities of aggregation observed by size exclusion chromatography correlate nicely with the predicted ranking of the T_m in each preservative case. This analysis of the microcalorimetric data justifies using the technique to correctly rank different formulations in terms of their predicted impact on aggregation. The evidence gathered supports the principles presented herein. However, so as not to misconstrue the importance of microcalorimetry, this technique, in combination with several other bioanalytical methods, can provide a powerful alliance in testing the scheme presented. For example, HPLC, SDS-PAGE, CD, and mass detection methods (i.e., AUC, light scattering, mass spectrometry) in conjunction with microcalorimetry can all participate in describing how the conformational state impacts the stability of a given biologic.

It has already been mentioned how high T_m's correlate with a lower susceptibility to aggregation and the preferred solution conditions in which M-CSF, IL-1R (types I and II), Flt3L, and CD40L are stabilized. Additionally, G-CSF

Table 13.1 Microcalorimetric Melting Temperatures of IL-1R (type I) and SEC *In Vitro* Stability Data at 37°C

				SEC			
	Microcalorimetry			7 d		60 d	
	T_m1 (C)	T_m2 (C)	T_m3 (C)	Agg (%)	Native (%)	Agg (%)	Native (%)
Control	50.8	53.7	66.3	0.66	98.93	1.50	97.54
0.065% phenol	50.3	53.4	66.5	1.02	98.62	3.07	96.02
0.1% *m*-cresol	48.4	51.9	65.8	1.37	98.25	5.10	93.92
0.9% benzyl alcohol	45.2	48.5	63.6	2.93	96.92	16.46	83.09

Note: Preservatives added to the same citrate formulation (20 m*M* sodium citrate, pH 6, and 100 m*M* NaCl).

Source: Data from Remmele, R.L., Jr., N.S. Nightlinger, S. Srinivasan, and W.R. Gombotz. 1998. Interleukin-1 receptor (IL-1R) liquid formulation development using differential scanning calorimetry. *Pharm Res* 15: 200–208.

(Neupogen), a four-helix bundle cytokine, is formulated at pH 4 but has been shown to maintain both thermal stability and tertiary structure at pH 2.[60] In fact, the secondary structure of this molecule was shown to remain highly helical at pH 4 (T_m approximately 62°C) and 2 (T_m approximately 63°C) as compared to pH 7 (T_m approximately 55°C) where a less conformationally stable form was observed. In the same study, FTIR and CD data corroborated the tendency of the protein to unfold as measured by the loss of helical structure in the order pH 7 > pH 4 > pH 2. Moreover, after determining optimal pH conditions of thermostability, several studies have shown that excipient screening at such conditions can successfully predict the rank of formulation cocktails that offer the most favorable stability.[14,23,31,56]

A number of examples have now been described where T_m has been shown to be a good parameter to indicate and rank appropriate stability. However, it is only one parameter in Equation 1 that is equated to conformational stability as described by ΔGu. It is important to remember that the current usage of T_m to confer stabilization is predicated upon the notion that high T_m's represent a greater resistance of the protein to unfold and that this behavior holds at lower temperatures where the protein is to be stored. Equation 1 permits a better understanding of the relationship of stability as a function of temperature that may not necessarily coincide with the paradigm so far outlined. In some cases, it may not be possible to accurately obtain the thermodynamic parameters that make the application of Equation 1 valid (e.g., non-two-state behavior). Furthermore, where parameters are measurable, maximal conditions of conformational stability may indicate more favorable free energies at low temperatures in the presence of some excipients that tend to lower the T_m. A listing of the thermodynamic parameters pertaining to several protein systems[34,38,39,61,62] that can be plugged into the modified Gibbs–Helmholtz equation are shown in Table 13.2. The thermodynamic behaviors of a few of these systems are plotted in Figure 13.8. Maximal conformational stability is achieved when the free energy difference between the native and denatured states is the greatest and positive. The compact native state is assumed to depict a state of lower energy than the denatured state.[63] Therefore, an enhancement of stability as a consequence of increasing the difference between these states by optimizing the solution conditions that make this possible is the premise for the microcalorimetric approach described in the preceding text. The temperature where this is true is called the temperature of maximum stability, or T_{ms}.[47] It is the point where the parabolic maximum occurs as described by the behavior shown in Figure 13.9.

Consider what happens to pepsinogen near its optimal T_m of 339.4°K (66.2°C), when 20% ethanol is added to the solution (Figure 13.9). The temperature of maximum stability occurs near 300°K (26.9°C). When 20% ethanol is added, the T_m is lowered to 329.0°K (55.9°C) as expected, suggesting some destabilization of the protein between the two solution conditions. However, the temperature of maximum stability occurs at a lower temperature near 273°K

Table 13.2 Thermodynamic Parameters of Different Protein Systems

Protein	Conditions	T_m (°K)	ΔH_m (kcal/mol)	ΔCp (kcal/mol-°K)	Ref.
α-Chymotrypsinogen (bovine)	pH 2.3	316.2	78	3.8	38
	pH 2.6	322.2	102	3.8	38
	pH 2.8	324.2	110	3.8	38
	pH 3.4	331.2	130	3.8	38
	pH 4.0	334.2	140	3.8	38
	pH 5.0	335.2	148	3.8	38
α-Chymotrypsin	pH 6.0	333.3	166	3.013	38
FGF-1 (human)	20 m*M* *N*-(2-acetamido)-iminodiacetic acid, 0.1 *M* NaCl, pH 6.6, with added 0.6 *M* GuHCl	315.7	73.04	0.608	34
	0.7 *M* GuHCl	312.6	61.50	1.554	34
	0.8 *M* GuHCl	310.1	56.02	1.995	34
	0.9 *M* GuHCl	307.0	47.08	2.360	34
	1.0 *M* GuHCl	304.8	41.09	2.193	34
	1.1 *M* GuHCl	299.9	29.42	2.428	34
Papain	pH 5	358.9	215.5	3.307	39
Pepsin	5 m*M* Na-phosphate and pH 6.5 (2 pks)	322.2	135	4.15	60
	pH 6.5 + 20% ethanol	312.0	227	2.77	60
	pH 5.0 + 20% ethanol	325.2	215	2.77	60
	pH 4.0 + 20% ethanol	332.7	233	2.77	60
	pH 3.0 + 20% ethanol	331.7	238	2.77	60
	pH 2.2 + 20% ethanol	329.2	212	2.77	60
	pH 2.0 + 20% ethanol	329.2	214	2.77	60
Pepsinogen	5 m*M* Na-phosphate and pH 6.0	339.4	254	5.8	61
	pH 6.4	336.0	248	5.8	61
	pH 7.2	329.3	195	5.8	61
	pH 7.7	328.2	173	5.8	61
	pH 8.0	324.3	182	5.8	61
	pH 5.9 + 20% ethanol	329.0	245	4.2	61
	pH 6.4 + 20% ethanol	325.3	248	4.2	61
	pH 6.8 + 20% ethanol	320.4	221	4.2	61
	pH 7.3 + 20% ethanol	313.0	192	4.2	61
	pH 8.0 + 20% ethanol	308.5	169	4.2	61
	pH 8.2 + 20% ethanol	307.0	170	4.2	61

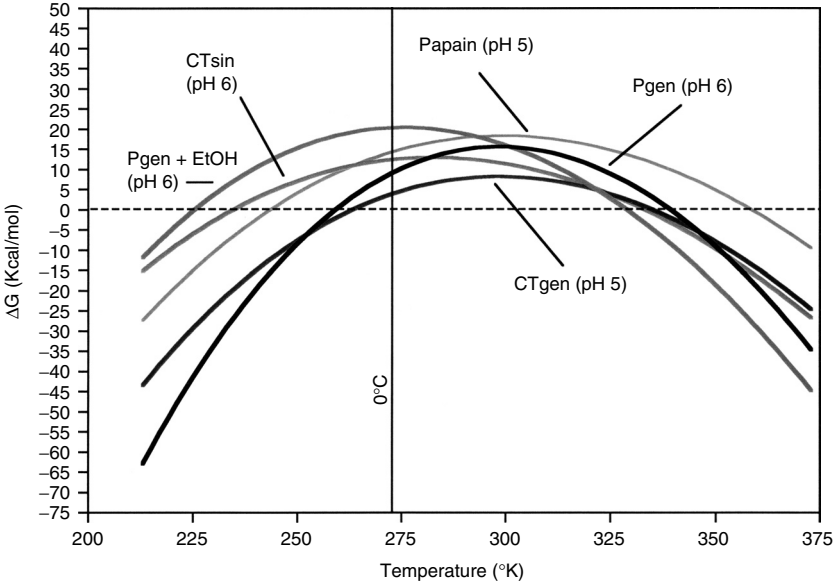

Figure 13.8 Temperature response trace (at optimal T_m solution conditions) of the free energy of unfolding (ΔGu), calculated from Equation 1. Pgen = pepsinogen, Ctsin = α-chymotrypsin, Ctgen = α-chymostrypsinogen, and papain. Note the pH conditions are listed in parentheses and the thermodynamic parameters used in Equation 1 are from those listed in Table 13.2.

(0°C) and indicates a greater ΔGu. Considering T_m alone, one might be inclined to think that the stability of this protein would be lower at conditions near 2 to 8°C. In fact, the cold denaturation temperature is also lowered, making this protein more stable in the presence of 20% ethanol at low temperature. This is something not readily apparent from T_m. It suggests that other excipients may produce similar behavior. Although not evaluated in this light, this could explain why the presence of polyethylene glycol (PEG) is somewhat more stabilizing at lower temperatures even though it exhibits a destabilizing shift in the T_m.[25] It should be pointed out that in both cases there was an observed change in the heat capacity term. In the case of pepsinogen with 20% ethanol, the ΔCp was lowered from 5.8 to 4.2 kcal/mol°K. A similar result was observed in the presence of PEG in terms of concentrations and molecular weight of the PEG added to various test protein systems analyzed.[25]

An explanation for these observances in the cases of ethanol and PEG may arise from hydrophobic interactions (i.e., methylene groups, methyl) with the unfolded state of the protein at elevated temperatures. This idea is supported by studies of the interaction of several alkylureas (methyl-, *N*,*N*dimethyl-, ethyl-, and butylureas) with the thermal unfolding of ribonuclease A, where it was shown

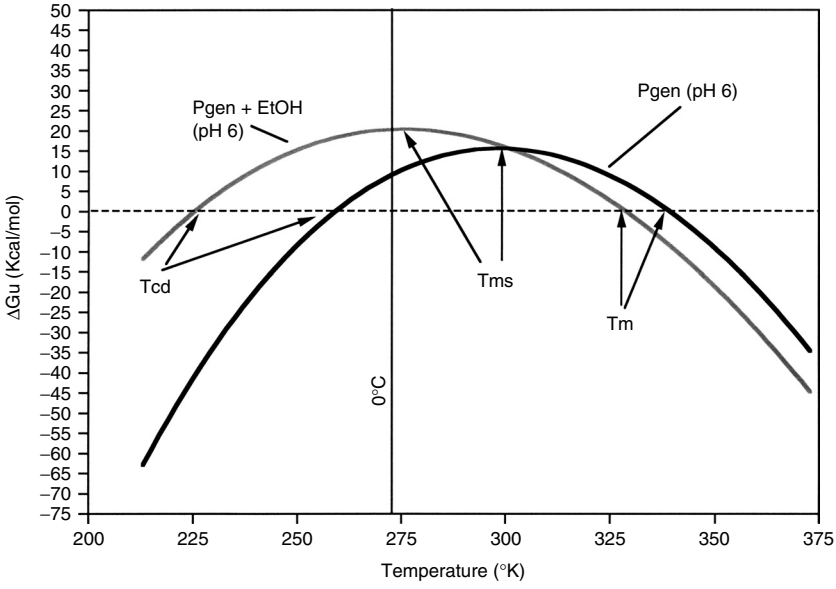

Figure 13.9 Temperature response trace (at optimal T_m solution conditions) of ΔGu, for pepsinogen at pH 6, with and without 20% ethanol (EtOH). Labels shown are identified as Tcd = cold denaturation temperature, T_{ms} = temperature of maximum stability, and T_m = melting transition temperature.

that the thermal stability of the protein decreased with increasing concentration and size of the hydrophobic group substituted on the urea molecule.[64] Another class of excipients commonly used in biopharmaceuticals are surfactants. They can afford significant stabilization at low temperatures during agitation where air–water interface reactions can lead to unfolding. However, they commonly result in lower T_m's that may stem from nonspecific interactions with solvent-exposed hydrophobic regions of the denatured protein at elevated temperatures.[65]

Protein Properties

Physical properties of the protein structure should be considered in designing strategies to achieve stable formulations because they can often yield clues about which solution environment would be appropriate for stabilization. For example, the insulin molecule is known to self-associate via a nonspecific hydrophobic mechanism.[66] Stabilizers tested include phenol derivatives, nonionic and ionic surfactants, polypropylene glycol, glycerol, and carbohydrates. The choice of using stabilizers that are amphiphilic in nature to minimize interactions where protein hydrophobic surfaces instigate the instability is founded upon the hydrophobic effect.[19] It has already been mentioned that hydrophobic surfaces prefer

to be buried in an aqueous environment (due to the unfavorable solvent entropic cost) and, therefore, will tend to associate in such a way as to remove the hydrophobic surface from the solvent and increase hydrophilicity. Hence, the hydrophobically exposed surface of the protein becomes "sticky" in such an environment.

The amphiphiles have both hydrophobic and hydrophilic properties that can interact favorably with the hydrophobic patches on the protein surface and also with the solvent, thereby reducing the propensity of forming aggregates. In fact, the covalent attachment of monosaccharides at strategic sites on the insulin molecule greatly improved the stability of this protein by hydrophilization of the hydrophobic surface area.[67] Moreover, glycosylation has been implicated to play an important role in stabilization, antigenicity, and biological function.[68] For example, aglycosylated and glycosylated forms of human IgG_1-Fc domains have been evaluated by microcalorimetry at pH 7.4 in a phosphate-buffered saline (PBS) solution. Two characteristic endothermic transitions with T_m of 65.2°C (assigned to C_H2) and 81.9°C (assigned to C_H3) were identified for the glycosylated sample in contrast to the deglycosylated form with shifts in the transition temperatures to 60.9°C and 68.1°C, respectively.[68] These data provide evidence of the importance of glycosylation for stabilization of the IgG-Fc. The same study also emphasized how glycosylation (localized at Asp297 on the C_H2 domain) affects structure required for FcγRI, FcγII, FcγRIII, and C1 binding and activation. It should be noted that the second transition of the Fc assigned to the C_H3 domain actually constitutes the melting of two domains (C_H3/C_H3) as a single cooperative block.[69] Furthermore, the C_H2 transition is accompanied by disruption of interdomain interactions (*cis* between C_H2 and C_H3 domains) that contribute to the high enthalpy of the first transition (57 kcal/mol) in contrast to the C_H3 transition (36 kcal/mol).[68,69] The afforded thermal stability of the glycan in this case bears a similar resemblance to the insulin case given that the IgG_1-Fc is predominantly hydrophobic. Salt in this case should benefit stabilization of the hydrophobic core.

Other studies of the role glycans play concerning protein stabilization suggest that deglycosylated forms exhibit lower thermostability as judged by a decrease in T_m and ΔH_m although not substantially affecting the conformation as indicated by far-UV CD.[70] In these latter studies, the thermal stability seemed to depend on the amount of glycosylation present (i.e., maximum stabilization was observed for the most heavily glycosylated protein, irrespective of the types, N-linked or O-linked, or patterns, mono- or multibranched, of the covalently attached carbohydrate chains). Additionally, it was shown that thermal reversibility of deglycosylated proteins was significantly diminished and that they were prone to aggregate in comparison to their glycosylated counterparts. Hence, glycosylation of recombinant proteins using appropriate expression vectors (i.e., CHO, yeast) can potentially afford improved stability (as described by microcalorimetric data) and robustness to withstand the stresses associated with the biopharmaceutical development train.

Understanding protein unfolding as it pertains to interactions with contact surfaces is also important to achieving a stable dosage form. Adsorption onto

container or device surfaces (i.e., syringes, vials, catheters) can lead to a loss of drug potency. In very dilute dosage forms, this can result in substantial differences between the expected concentration and that delivered to the patient. Microcalorimetry has been used successfully to quantify losses in secondary structure of globular proteins upon adsorption to solids.[71] For example, the T_m, $\Delta H_{P\text{-}D}$, $\Delta H_{N\text{-}D}$, and $\Delta Cp_{P\text{-}D}$ were all determined (where the subscripts P = adsorbed perturbed state, N = native, D = denatured). The magnitude of the $\Delta H_{P\text{-}D}$ relative to the $\Delta H_{N\text{-}D}$ was used as an unambiguous gauge of the extent of secondary structure loss in proteins as a result of adsorption. The high T_m was indicative of a highly stable adsorbed-state structure. Examination of lysozyme adsorption to polystyrene latex and hematite revealed that it adsorbed irreversibly, yet the extent of the unfolded structure was less for hematite than for polystyrene latex. This comparison indicated that lysozyme retained most of its native structure when adsorbed to a more hydrophilic surface. Studies of this kind make it possible for one to not only obtain a better understanding of the thermodynamics of protein adsorption, but also allow one to delineate between solid surfaces where the protein is less susceptible to adsorb.

Most of what has been presented has dealt with the propensity of the unfolded state to form aggregates. However, deamidation reactions can also be affected by the conformational flexibility of the protein in the vicinity of Asn residues.[15,72] Protein sequences possessing Asn-Gly are particularly labile as a result of decreased steric hindrance associated with the lack of a side chain on the Gly residue that allows free rotation of the asparaginyl side chain to permit nucleophilic attack from the peptide bond nitrogen forming a cyclic imide intermediate. This intermediate is particularly unstable toward hydrolysis, leading to the formation of a mixture of α- and β-aspartyl residues, which may affect the efficacy of the drug. Deamidation studies at pH 7 of polyanion-stabilized (heparin) acidic fibroblast growth factor (aFGF) have revealed that, among the three Asn sites located near the N-terminus (Asn3-Leu4, Asn8-Tyr9, and Asn19-Gly20), only the Asn8-Tyr9 deamidated.[72] The unexpected absence of deamidation at the notoriously labile Asn19-Gly20 suggested that there was no simple correlation between local amino acid sequence, conformational flexibility, and deamidation potential. Yet an explanation offered for this anomalous result was that the Asn19-Gly20 site was involved in heparin binding, thus permitting greater conformational rigidity and affording some protection against deamidation. It should be pointed out that heparin had been shown to stabilize aFGF against thermal, pH, and proteolytic degradation.[72] This example illustrates how binding a particular substrate to a protein can sometimes increase stabilization of chemically labile residues.

Folding and Stability

Structural factors are important regarding rational design approaches that lead to predicting stable protein folds. Can anything be learned about protein stability from different structural elements, amino acids, and packing of the native folds

common for most protein systems? The answer to this important question is yes! Efforts to understand the tendencies of amino acids in peptides to contribute to ordered and disordered structure have been and continue to be examined. For example, scales based upon probabilities associated with a given amino acid's contribution to structure in a peptide segment have been used to classify amino acids from order-promoting to disorder-promoting in the following manner: Trp > Phe > Ile > Tyr > Val > Leu > Cys > Met > Ala > Asn > Thr > Arg > His > Gly > Asp > Ser > Gln > Glu > Lys > Pro.[73] Using such an index, one would expect tryptophan to have a high probability as an order-promoting amino acid in contrast to proline that would be disorder promoting. Deciphering the role of each amino acid as it pertains to fold recognition requires an understanding of the thermodynamic tendency of each amino acid to stabilize native-state ensembles. It has been observed that amino acid types partition unequally into high, medium, and low thermodynamic stability environments and suggest that calculated thermodynamic stability profiles have the potential to encode sequence information.[74] In this context, 44 nonhomologous proteins were analyzed using the COREX algorithm[75] where energy differences between each partially unfolded microstate and fully folded reference state were determined by the energetic contributions of all amino acids comprising the folding units that unfolded in each microstate, plus the energetic contributions associated with exposing additional (complementary) surface area on the protein. This can be described by the equation $\Delta ASA_{total} = (ASA_{unf} + ASA_{comp}) - (ASA_{native})$. The results suggested that aromatic amino acids Phe, Trp, and Tyr are mostly found in high-stability environments, whereas Gly and Pro were overwhelmingly found in low-stability environments. This was in contrast to amino acid residues such as Ala, Met, and Ser that showed distributions not significantly different from the randomized data. Additional studies using computational methods to test different combinations of secondary structure fragments of 240 nonhomologous proteins have shown that an overwhelming majority can be successfully recognized by the energies of interaction between residues of secondary structure.[76] The results of this study found that β-structures contributed more significantly to fold recognition than α-helices or loops. Additionally, it has been shown from studies of unfolding thermodynamics of the all β-sheet structure of interleukin-1β that the Gibbs free energy of a hydrogen bond in the β-sheet structure is greater than in α-helices.[77]

In a different study, a 29-residue dicyclic helical peptide, shown to be two-state, thermally reversible, and to unfold in a cooperative manner within the temperature range extending from 10 to 100°C, was intentionally designed with side-chain to side-chain covalent links at each terminal to stabilize the helix structure.[78] Complete thermodynamic characterization of helix unfolding could then be examined. Unfolding was found to proceed with a small positive heat capacity increment, consistent with the solvation of nonpolar (hydrophobic) groups upon unfolding. The conclusion was that hydrogen bonds were not the only factors responsible for the formation of the α-helix, but that hydrophobic

interactions also contributed to its stabilization. At 30°C, the calorimetric enthalpy and entropy values were estimated to be 18.85 (±1.45) kcal/mol and 58 (±5.8) cal/mol-°K, respectively. With regard to protein systems, human plasma apolipoprotein A-2 (apoA-2) also unfolds reversibly and has an enthalpy of unfolding of 17 (±2) kcal/mol for helical structure.[79] Thermal unfolding of γγ and ββ homodimeric coiled-coils of tropomyosin exhibit multistate unfolding properties with overall unfolding enthalpies near 300 kcal/mol.[80] The electrostatic stabilization effects of coiled-coils have been investigated using a sequence shuffling strategy without changing the overall content of amino acids in the peptides, and have shown that in solutions of low ionic strength, ionic pairs contribute significantly to the stability of the coiled-coil conformation.[81]

Structure stabilization of protein systems has also focused on design parameters of the protein's core. In one such study, the hydrophobic core of a four-helix bundle protein, Rop, was altered mutagenically to study packing patterns and various side-chain shapes and sizes as it related to properties of stabilization and destabilization.[82] It was discovered that overpacking the core with larger side chains caused a loss of native-like fold, decreasing the associated thermal stability of the molecule. This study defined the role of tight residue packing and burial of hydrophobic surface area in the construction of compact native-like proteins. Solvent influences on hydration properties of protein secondary structures have also been evaluated, indicating that the strength of water binding to carbonyl groups is lower for β-sheet proteins than in α-helical proteins, owing to the differences in the geometry of the water carbonyl group interactions.[83]

What structural properties are necessary to make a protein thermally stable? Much of what is currently known comes from examination of structural properties of hyperthermophilic and thermophilic proteins. At high-temperature conditions where many proteins from mesophilic organisms would naturally denature, hyperthermophilic proteins thrive and exhibit higher T_m. Clues to answer the question may be obtained by comparing the structural fingerprint features of mesophilic proteins to those of the hyperthermophilic class. For example, the structure of the hyperthermophilic tungstopterin enzyme, aldehyde ferredoxin oxidoreductase, has a relatively small solvent-exposed surface area and a relatively large number of both ion pairs and buried atoms.[84] The ion pairs constitute salt bridges between acidic amino acids (i.e., aspartic and glutamic acids) and the basic amino acids (i.e., arginine, histidine, and lysine).

In another study of *Thermus aquaticus* D-glyceraldehyde-3-phosphate dehydrogenase, among the various structural factors evaluated (i.e., salt bridges, hydrogen bonds, buried surface area, packing density, surface-to-volume ratio, stabilization of α-helices and β-turns), a strong correlation between thermostability and the number of hydrogen bonds between charged side chains and neutral partners was discovered.[85] Charge-neutral hydrogen bonds were believed to provide electrostatic stabilization without the heavy desolvation penalty of salt bridges. What is interesting concerning ΔGu of mesophilic and thermophilic proteins is the fact that the free energy for thermophiles is not much larger than

that of the mesophiles, essentially equivalent to a few hydrogen bonds or ion pairs. Oligomerization of the protein has also been cited as a means for *Thermus thermophilus* pyrophosphatase stability in which it is tightly packed, having a rigid structure, and comprising hydrogen bond and ionic interactions that form an interlocking network which covers all of the oligomeric surfaces.[86] This in turn translates into an increase in buried surface area upon oligomerization by about 16%.

Recently, investigation of how proteins are packed has led to the idea that although they have average packing densities as high as crystalline solids, they look more like liquids or glasses by their free volume distributions.[87] Moreover, the distributions are broad and indicate that the interiors may better be described as randomly packed spheres where larger proteins are packed more loosely than smaller proteins. Citrate synthase from hyperthermophilic archeon *Pyrococcus furiosus* (an organism that optimally grows at 100°C) was compared to mesophilic and thermophilic versions of the same protein. The most significant feature was an increased compactness of the enzyme, a more intimate association of the subunits (homodimer), an increase in intersubunit ion pairs, and a reduction of thermolabile residues.[88] Compactness was achieved by shortening the number of loops, increasing the number of buried atoms in the core, and optimizing the packing of side chains in the interior, resulting in a reduction of cavities. A common thread emerges concerning each of these investigations, namely, thermal stability is related to a native compact structure that involves an enhancement of hydrogen bonding, packing density, and salt bridges that are important to the protein fold.

Finally, assimilating information about the structural properties of a given biologic, combined with microcalorimetric data about stabilizing solution environments and the results of accelerated studies to characterize major instabilities (i.e., aggregation, deamidation, oxidation, proteolysis, hydrolysis), it should be possible to select respectable candidate solutions to evaluate in real time to determine achievable longevity. The approaches outlined in this section are suggested as a guide in the preformulation and formulation development design. They have been shown to work well in some cases presented. Currently, there is no acceptable way of predicting the real-time shelf-life apart from carrying out real-time studies. However, there have been attempts to characterize degradation products using activation energies obtained from reactions that follow Arrhenius behavior that have met some measure of success.[13,89,90] This subject will be discussed in more detail in a following section.

ISOTHERMAL TITRATION CALORIMETRY (ITC)

The study of protein function as it applies to covalent and noncovalent molecular changes associated with specific binding is of fundamental interest to those involved with the discovery of therapeutic proteins. Discovering soluble receptors that bind the cytokines that elicit inflammatory immune responses is one of many

approaches to treating physical disorders (i.e., rheumatoid arthritis, asthma). In such cases where intermolecular recognition is to be characterized, the ITC technique can offer some advantages. This technique is capable of thermodynamic characterization of the binding affinities of new drugs that act as receptors, antagonists, or agonists of biological function. It has been acclaimed to rival most alternative methods used to acquire information of this kind (i.e., enzyme-linked immunosorbent assays, absorption and fluorescence spectroscopy, magnetic resonance, chromatography, etc.). Although radiolabeling techniques and plasmon resonance methods (e.g., BIAcore) are capable of obtaining data at lower concentrations than microcalorimetry, they are not necessarily superior techniques for measuring binding constants. Among the true "in-solution" methods that do not require protein modification (i.e., ITC and analytical ultracentrifugation), only ITC can provide a complete thermodynamic characterization of the system under study.[91] This is an important advantage when comparing results to BIAcore techniques in that binding reactions that exhibit entropy/enthalpy compensation often yield free energies of binding that exhibit little change.[53] An understanding of whether entropy or enthalpy drives the reaction can be very important yet not obvious from the free-energy parameter obtained from the on/off rate equilibrium constants typically obtained from BIAcore measurements. In enthalpy-driven reactions, the enthalpy is large, and the entropy component of the reaction is unfavorable (negative). The inverse is generally true for entropy-driven reactions. In situations in which a reaction is enthalpy driven, a loss of conformational mobility may result upon binding. Alternatively, reactions that are entropy driven may suggest that hydrophobic contacts remove hydrophobic surface area from the water environment, thereby increasing entropy of the solvent upon binding. As for binding constant comparisons between the BIAcore and ITC, there have been studies that would indicate that the two methods yield similar results.[92]

Protein–Ligand Interactions

Just like conventional scanning microcalorimetry, the liberation and absorption of heat associated with the chemical reaction are measured in an ITC experiment. However, in this case, the heat is due to a reaction involving binding between the protein and a ligand. The ligand may be either another protein, nucleic acid, lipid, or a small molecule. It is the only method that is capable of determining ΔG_b, ΔH_b, and ΔS_b of binding (subscript b denotes binding), the binding constant (Ka) and stoichiometry (N), in a single experiment.[91] Additionally, background interferences commonly observed in optical absorption or fluorescence methods (where solution components may also have absorption, fluorescence, or scattering properties) are normally very low in ITC experiments, which permits the study of heterogenous mixtures.

In principle, the experiment is carried out at constant temperature by titrating one binding partner into a solution containing the other in the sample cell of the calorimeter. After a small increment of titrant is added to the sample cell, the

heat liberated or adsorbed in the sample cell is quantitatively measured with respect to a reference cell filled with the identical solution without protein. The change in heat is the electrical power required to maintain a constant temperature between the sample and reference cells. Upon continued titration, the enthalpic response decreases until saturation is achieved. The contents of the cell are stirred continuously during the experiment by the spinning motion of the syringe-paddle from which the titrant is dispensed to achieve rapid equilibrium between the reagents.

An example of such a titration is illustrated in Figure 13.10, where 0.061 m*M* RNase A in the sample compartment was titrated with 2.13 m*M* 2′CMP (titrant). In the upper panel, the heat signal shown by the downward directional peaks are exotherms of the reaction mixture. In a typical experiment, the total heat of each injection of titrant is computed as the area of the downward peak. When the total heat is plotted against the molar ratio of ligand (2′CMP) added to the sample (RNase A) as depicted in the lower panel of the figure, one obtains the complete binding isotherm. This experiment was performed using a MicroCal VP-ITC system with accompanying software containing the algorithms to compute the stoichiometry of binding, the binding constant, and enthalpy of binding. The free energy of binding may then be determined by the equation $\Delta G_b = -RT \ln Ka$, where R is the gas constant and T is the absolute temperature. The entropy can be indirectly determined using the Gibbs–Helmholtz expression ($\Delta G_b = \Delta H_b - T\Delta S_b$) once ΔG_b is calculated from Ka. In this case, $\Delta G_b = -8.07$ kcal/mol. Saturation occurs when the heat signal becomes small, approximating the heat of dilution of the titrant into the sample. This is the case in the example presented when the mole ratio exceeds 2.5 (Figure 13.10). This technique can be a powerful tool used in conjunction with scanning microcalorimetry for characterizing a given protein biologic.[53]

One limitation of this technique is that the largest binding constants that may be reliably measured are about $10^9\ M^{-1}$ for typical protein–ligand interactions.[93] Options to get around this issue involve experiments conducted at different pH or temperature conditions in which the binding constant may be evaluated with greater ease. Although this approach can be useful in acquiring information about linked protonation effects, the observed binding enthalpy and heat capacity change can undergo extreme deviations from their intrinsic values depending upon pH and buffer conditions.[94] There could be concerns regarding the value at physiological conditions where the protein biologic is expected to be efficacious. Alternatively, competitive binding by titration displacement schemes may be applied to estimate tight binding affinities that are greater than $10^9\ M^{-1}$.[95] However, even with this approach there is a possibility of error and added complexity associated with the reaction. Recently, competitive binding by displacement titration has been improved using cubic binding equations that may allow for greater accuracy for very tight binding reactions.[96] Such an approach requires independent experiments with a competitive binding inhibitor that is a few orders of

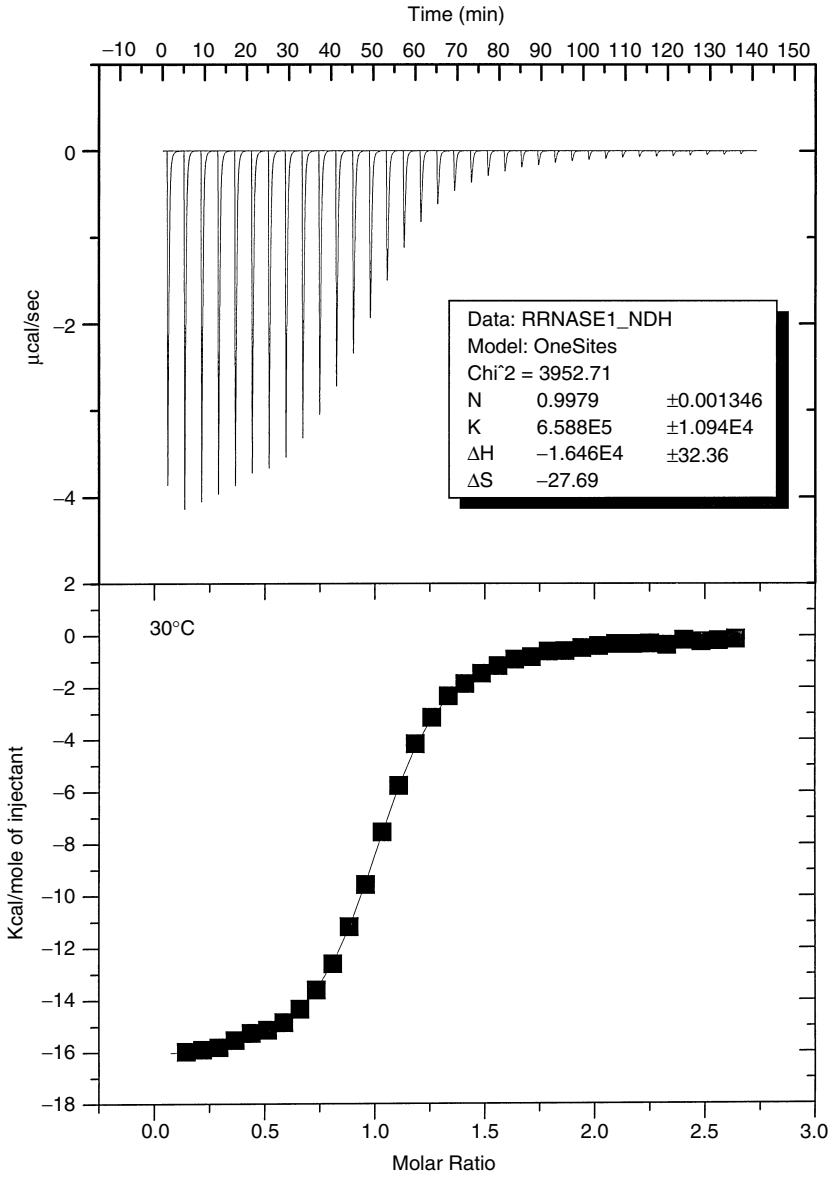

Figure 13.10 Calorimetric titration response showing the exothermic raw (downward-projecting peaks, upper panel) heats of the binding reaction over a series of injections titrating 0.061 m*M* RNase A (sample) with 2.13 m*M* 2CMP at 30°C. Bottom panel shows the binding isotherm obtained by plotting the areas under the peaks in the upper panel against the molar ratio of titrant added. The thermodynamic parameters were estimated (shown in the inlay of the upper panel) from a fit of the binding isotherm.

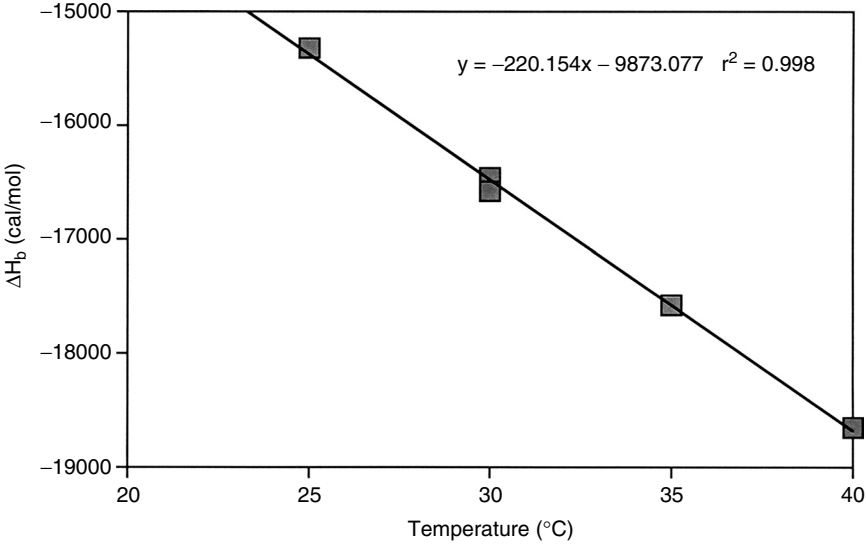

Figure 13.11 A plot of the enthalpy of binding (ΔH_b) as a function of temperature for the RNase A/2CMP system. From the slope of the line shown, one obtains the ΔCp_b of the reaction.

magnitude lower than the tight binding interaction of interest. Despite the shortcomings, a variety of interesting reactions have been studied.

It is also possible to estimate binding constants much greater than $10^{10}\ M^{-1}$, using more conventional DSC methods that mathematically model protein–protein or protein–ligand interactions, resulting in perturbations that affect the T_m.[97] This approach has been shown to exhibit agreement when binding sites are completely saturated, but can result in substantial errors when site saturation is incomplete and the transition of ligand molecules overlaps that of unliganded molecules.

The heat capacity of binding (ΔCp_b) may be determined by plotting the ΔH_b as a function of temperature. Such a plot is illustrated in Figure 13.11 for the 2′CMP binding to RNase A example. A ΔCp_b of –220 cal/mol-°K indicates a complex that has a smaller heat capacity than the sum of its free components, corresponding to the changes in the degree of surface hydration in the free and complexed forms.[53] Results from liquid hydrocarbon transfer and solid dissolution experiments support the idea that polar and nonpolar interactions differ in the sign of the change in heat capacity.[98] Hence, mutation studies that weaken hydrophobic contributions of the complex form of the protein would be expected to make ΔCp_b less negative. Conversely, decreasing polar interactions would necessarily make ΔCp_b more negative. For example, the ΔCp_b values for a triple alanine mutant (–927 cal/mol-°K) of the human growth hormone (hGH)–receptor

interface was shown to be significantly more negative than the ΔCp_b for the wild-type interaction (–767 cal/mol-°K).[99] Such negative ΔCp_b values are consistent with the proposal that the hydrophobic effect is the primary contributor to the free energy of binding at the protein complex interface.

In the development of a biopharmaceutical, it is often desirable to determine binding affinities of a target protein–ligand system. Despite the shortcomings associated with binding affinities within a narrow range ($\leq 10^9\ M^{-1}$ and $\geq 10^3\ M^{-1}$), many systems can be directly evaluated by this technique. The remaining discussion will focus on some of the work that has been performed looking at protein–ligand interactions using ITC, where the ligand may be a receptor, an antigen, an antibody, a carbohydrate, or a lipid.

Receptors

This technology is particularly well suited for the characterization and study of protein design factors as they affect stability and binding to different receptors. For example, receptor dimerization has been considered a primary signaling event during binding of a growth factor to its receptor at the cell surface. Analysis of binding epidermal growth factor (EGF) to the extracellular domain of its receptor (sEGFR) has been performed using ITC.[100] The data indicated the stoichiometry of binding to be one EGF monomer bound to one sEGFR monomer followed by dimerization of two monomeric (1:1) EGF–sEGFR complexes. Rational mutagenic approaches involving the modification of protein binding sites to acquire a biophysical understanding of the protein engineered changes that modulate binding affinities in solution phases have been performed on a number of systems.[99–104] For example, the homopentameric B subunit of vertoxin 1 (VT1) binds to the glycosphingolipid receptor globotriaosylceramide (Gb_3). Mutants with alanine substitutions near the cleft between adjacent subunits were studied to understand the effects of binding affinity.[102] Substitution of alanine with phenylalanine (Phe-30) resulted in a fourfold reduction in binding affinity for Gb_3. Examination of the binding of VT1 subunit B with trisaccharide in solution by ITC showed that the Phe-30 mutant was markedly impaired in comparison to the wild type and too weak to calculate the binding constant. To ensure that the mutant did not undergo a significant change in structure, it was crystallized and evaluated by x-ray diffraction. The data showed that the structure was in fact identical to the wild type except for the Ala30Phe substitution. This evidence suggested that the aromatic ring of Phe-30 greatly affected the binding to the Gala1–4Galp1–4Glc trisaccharide portion of Gb3.[101] In another mutagenesis study of the contact side chains in the hGH–receptor interface, a triple mutant comprised of Phe25Ala, Tyr42Ala, and Gln46Ala was evaluated by ITC.[99] Binding kinetics of the triple-alanine mutant showed that neither association nor dissociation rates were significantly affected, and only slight local disorder was seen in the crystal structure. However, ITC showed large and compensating changes in the enthalpy and entropy of binding. The triple mutant bound with a

favorable enthalpy of ΔH_b = –12.2 kcal/mol and a corresponding less favorable entropy of ΔS_b = –2.3 cal/mol-°K in comparison to the wild type of ΔH_b = –9.4 kcal/mol and ΔS_b = 7.7 cal/mol-°K. Dissection of the triple-alanine mutant into single Phe25Ala and double Tyr42Ala/Gln46Ala mutants showed that the more favorable enthalpy was derived from the removal of the Phe-25 side chain on helix-1 of the hormone. These results demonstrate that multiple-alanine mutations at contact residues may not affect binding kinetics, affinity, or global structure, yet they produced local structural changes that cause large compensating effects on the entropy of binding.

In another study, the thermodynamics of the binding of cyclic adenosine monophosphate (cAMP) and its nonfunctional analog, cyclic guanosine monophosphate (cGMP), to cyclic AMP receptor protein (CRP) and its Thr127Leu mutant were investigated by ITC at 24°C and 39°C.[102] The binding of the first cAMP molecule to CRP was found to be exothermic. However, successive binding of cAMP to CRP was endothermic and cooperative, indicating that the binding of the first cAMP molecule increased the affinity for the second one by more than an order of magnitude at 24°C. In the same study, it was shown that the overall binding of cGMP to CRP was exothermic and noncooperative. The point mutation of Thr127Leu switched off the cooperativity between cAMP-ligated binding sites without affecting the binding constant of cAMP and changed the specificity of the protein so that transcription was activated only upon cGMP binding. All of the binding reactions to CRP and the mutant were found to be entropically driven at 24°C.

The principal loci for binding interactions between aspartate and serine receptors of *E. coli* and methytransferase has been investigated and found to involve the last five amino acids of the receptor.[104] Truncation experiments performed on the C-terminal fragments of an aspartate receptor involving either the last 297, 88, or 38 amino acids gave comparable values of binding by ITC (N = 1, $\Delta H_b \sim 13$ kcal/mol, and Ka $\sim 4 \times 10^5$ M^{-1}). Truncating either 16 or 36 amino acids from the C-terminus eliminated detectable interactions. In the same study, a pentapeptide consisting of Asn-Trp-Glu-Thr-Phe (corresponding to the last five amino acids of the receptor and conserved in *E. coli* serine and aspartate receptors and also in the *Salmonella typhimurium* aspartate receptor) was found to have complete binding activity of the full-length receptor and the C-terminal fragments. In an *in vitro* methylation assay, this peptide was able to completely block receptor methylation.

The ITC technique was used to show that aFGF forms a 1:1 complex with the soluble extracellular domain of the FGF receptor (sFGFR).[103]. At 25°C, the Ka of this reaction was shown to be approximately 1.89×10^6 M^{-1} (ΔH_b = –5.3 kcal/mol). This binding reaction exhibits a favorable binding entropy (ΔS_b = 10.93 cal/mol-°K), perhaps indicating that hydrophobic surface area is removed from the solvent phase upon binding. As mentioned earlier, the labile Asn19–Gly20 linkage of this molecule does not deamidate appreciably when liganded to a stabilizing polyanion (i.e., heparin, sulfated β-cyclodextrin, sucrose octasulfate).

The stoichiometry for the binding reactions of 4.8 kD heparin was found to be about 4:1 (aFGF:heparin); of 16 kD heparin, 11:1 (aFGF:heparin); and for sucrose octasulfate, 1:1 (aFGF:sucrose octasulfate). Binding affinities for the same reactions were approximately $2.17 \times 10^6\ M^{-1}$ ($\Delta H_b = -4.8$ kcal/mol), $1.98 \times 10^6\ M^{-1}$ ($\Delta H_b = -5.1$ kcal/mol) and $0.294 \times 10^6\ M^{-1}$ ($\Delta H_b = -5.8$ kcal/mol), respectively. Hence, the binding affinities for both heparin treatments were essentially the same as that for the sFGFR with comparable enthalpies of binding. However, sucrose octasulfate, showing comparable enthalpy of binding, exhibited a weaker binding affinity with a less favorable ΔS_b (5.56 cal/mol-°K), suggesting that less hydrophobic surface area was buried in the complex. This study indicates the potential use of ITC to evaluate excipients that bind a given drug, realizing that in this particular case, stabilization against deamidation was minimized by adding an appropriate substrate that could bind to aFGF.

Antibodies

Considerable progress has been made regarding the design of antibodies that target a given disease.[98] A fundamental aspect involves an improved understanding of the forces surrounding the high affinity and specificity of antibody–antigen interactions. To this end, thermodynamic characterization is essential for improving protein design and deriving structural and functional information about binding. The role of hydrogen bonding and solvent structure as it pertains to the removal of specific hydrogen bonds in an antigen–antibody interface of three Fv (antibody fragment consisting of the variable domains of the heavy and light chains) mutants complexed with lysozyme has been examined using ITC.[105] The thermodynamic parameters for a series of mutants indicate a $Ka = 2.6 \times 10^7\ M^{-1}$ for a VL-Tyr50Ser mutant (where VL represents the variable light chain portion of the antibody), $Ka = 7.0 \times 10^7\ M^{-1}$ for a VH-Tyr32Ala mutant (where VH represents the variable heavy chain portion of the antibody), and $Ka = 4.0 \times 10^6\ M^{-1}$ for the VH-Tyr101Phe mutant. All mutants yielded binding constants that were less than the WT complex ($Ka = 2.7 \times 10^8\ M^{-1}$). In each mutant case, entropy compensation was attributed to the affinity losses. This study provided evidence that the complex was considerably tolerant, both structurally and thermodynamically, to the removal of antibody side chains that form hydrogen bonds with the antigen because the absence of these hydrogen bond sites resulted in minimal shifts in the positions of the remaining protein atoms. Furthermore, modified Fv fragments of antilysozyme monoclonal antibodies have been characterized using ITC.[105–109] Both enthalpy- and entropy-driven binding reactions have been observed. X-ray diffraction data at 2.5-Å resolution indicated that conformational changes of several D1.3 (antilysozyme monoclonal antibody) contacting residues located in the complimentary determining regions might explain the entropy-driven binding observed.[106] In another study, thermodynamic characterization of variable domains linked covalently with a flexible linker yielded constructs with reduced activity in comparison to the Fv of the monoclonal antibody (HyHEL10)

that was attributed to a loss of entropy upon antigen binding.[107] Mutagenic experiments of the antigen hen egg white lysozyme (HEL) and its binding affinity to HyHEL10 confirmed experimentally that structural perturbations involving the rotation of Trp-62 of HEL contributed to the gain in enthalpic energy upon binding to the antibody, even though it was proposed not to be in direct contact.[108] Tyrosine fragments have been mutated on the HyHEL10 antibody to show that the role of Tyr residues contributed to formation of hydrogen bonds through the hydroxyl group, permitting more favorable interactions through the aromatic ring and less entropic loss upon binding.[109]

Purification steps involving columns packed with protein A resin are often used to bind and elute proteins possessing IgG Fc domains (i.e., antibody fusion proteins, antibodies). Protein A has five immunoglobulin binding domains, identified as domains A–E. Thermodynamic characterization of the Fc binding and localization of the Fv-binding site to domains of protein A were evaluated by ITC.[110] Analysis of the binding isotherms obtained for the titration of hu4D5 antibody Fab fragment (containing the antigen-binding site) with intact full-length protein A indicated that three to four of the five domains can simultaneously bind to Fab with an approximate binding affinity of $5.5 \times 10^5\ M^{-1}$. Both D and E domains can functionally bind hu4D5 Fab fragments. Thermodynamic parameters for the titration of the E domain with hu4D5 Fab were found to be N = 1, Ka = $2.0 \times 10^5\ M^{-1}$, ΔG_b = –7.228 kcal/mol, ΔH_b = –7.1 kcal/mol, ΔS_b = –0.4298 cal/mol-°K.

Protein/Carbohydrate

Developing a better understanding of how to manipulate the cellular machinery to engineer the desired carbohydrate composition of cellular proteins is currently being considered.[111] This process utilizes a substrate-based approach in which novel cellular properties such as complex carbohydrates may be engineered by using analogs of small-molecule metabolites instead of relying on the manipulation of enzymes that process such compounds. Because it has already been mentioned that carbohydrates can structurally play a role concerning stability and recognition, such an approach could be quite valuable in the development of more robust biopharmaceuticals.

Chemokines selectively recruit and activate a variety of cells during inflammation. Chemokines bind glucosaminoglycans (GAGs) on human umbilical vein endothelial cells with affinities in the μmolar range ($10^6\ M^{-1}$): RANTES > MCP-1 > IL-8 > MIP-1α.[112] Isothermal titration calorimetry was used to confirm that this binding depended upon the length of GAG fragment and optimally required both N- and O-sulfation.[112] Suffice to say that GAG–protein interactions regulate myriad physiologic and pathologic processes. Yet our structural understanding of such binding reactions has been found lacking. Heparin is an example of a GAG that interacts with proteins, yet the general structural requirements for protein or peptide–GAG interaction have not been well characterized. Study of the nature

of electrostatic interactions between sulfate and carboxylate groups of GAG and basic amino acid residues in protein or peptides (i.e., arginine, lysine) has been carried out using ITC.[113] The results of blocked- and unblocked-charge experiments suggested that arginine-containing peptides bound more tightly to GAGs than the analogous lysine species owing to a high affinity of the guanidino cation to the sulfate anion of GAGs. This interaction was thought to originate from the combination of stronger hydrogen-bonding and exothermic response related to the electrostatic association between the arginine side chain and the glycan.

Close examination of the spacing of arginine and lysine residues as it pertained to heparin-binding sites revealed that binding affinity varied directly with arginine enrichment in a set of peptide sequences tested by ITC.[114] Given the high affinity of peptides of this kind, long stretches of basic amino acids are uncommon in heparin-binding proteins. Protein-binding sites commonly contain single isolated basic amino acids separated by one nonbasic amino acid. Comparisons between heparin (highly sulfated) and heparan (with fewer and greatly spaced sulfate groups) showed that both interact with complimentary peptide side chains that most appropriately reflect the same spacing among basic amino acids.[114] Hence, in contrast to heparin, heparan interacted most tightly with peptides with more widely spaced cationic residues. As a side note regarding the importance of appropriately positioned cationic charge to augment the binding interaction between protein and heparin, it has also been demonstrated that the removal of such charged side chains by replacement with alanine has deleterious consequences on heparin binding.[115] Collectively, this knowledge may be used to modulate the affinity of protein binding to heparin and to design effective peptide inhibitors to act as antagonists to frustrate protein–GAG interactions in some situations.

Serum-type and liver-type mannose-binding proteins (MBP) found in higher animals are composed of a carbohydrate-recognition domain (CRD) and a collagenous domain. These proteins can bind *N*-acetylglucosamine and other related sugars. The substrate preference of CRDs has been investigated and found to show little discrimination among monosaccharide specificities of the CRDs of the two different MBPs.[116] However, there are notable differences for the affinities of natural glycoproteins and mannose-containing cluster glycosides. Synthetic cluster ligands with two terminal GlcNAc moieties have affinities equal to monovalent GlcNac ligands of both CRDs, whereas a series of structurally similar mannose terminal divalent ligands displayed about 20-fold enhanced affinity for the liver-type CRD exclusively. An explanation for this observation is that liver MBP-CRDs have two sugar-binding sites per subunit, one of which only binds mannose, and the other both mannose and *N*-acetylglucosamine. In contrast, the serum MBP-CRD has only one site of the latter type. These findings were confirmed by ITC measurements.

The thermodynamics of the maltose-binding protein of *E. coli* (MalE) have been studied using both DSC and ITC.[117] This protein is a periplasmic component of the transport system for malto-oligosaccharides and is used widely as a carrier

protein for the production of recombinant fusion proteins. The MalE protein was shown to exhibit a ΔHcal/ΔHv ratio of 1.3 to 1.5, suggesting that the endotherm of unfolding comprises two strongly interacting thermodynamic domains. Binding of maltose resulted in an increase of the T_m by 8 to 15°C, depending on pH. The binding of maltose to MalE is characterized by very low enthalpy changes (on the order of 1 kcal/mol). Thermal melting of MalE was found to be accompanied by an exceptionally large change in heat capacity, consistent with a large amount of nonpolar surface area, approximately 0.72 $Å^2$/g protein that becomes accessible to the solvent in the unfolded state. It is worth noting that the high ΔCp determines a very steep ΔG vs. temperature profile for this protein and predicts that cold denaturation should occur above freezing temperatures. In fact, evidence for this was provided by changes in fluorescence intensity upon cooling the protein, showing a sigmoidal cooperative transition with a midpoint near 5°C at low pH conditions.[117] Furthermore, analysis of several fusion proteins containing MalE have illustrated the feasibility of assessing the folding integrity of recombinant products prior to separating them from the MalE carrier protein.

Protein and Lipid

Typical ranges for the binding affinities of proteins with lipids or fatty acids range from 10^3 to 10^6 M^{-1}. This is well within the range of direct detection using ITC. The binding of neuropeptide substance P (SP) agonist to lipid membranes and to neurokinin-1 (NK-1) receptor is one example.[118] The rationale of the study was to correlate the physical-chemical properties of three different SP analogs with lipid-induced conformation and membrane-binding affinity, and with receptor binding and functional activity. Hence, one analog was made more hydrophilic at the C-terminus with an (Arg9)SP or more hydrophobic in the (Nle9)SP form. The third analog was made with a reduced charge at the N-terminal address (AcPro2, Arg9)SP. In solution, all three analogs exhibited random coil conformations as confirmed, using circular dichroism. Addition of SDS micelles and negatively charged vesicles induced partially α-helical structures for (AcPro2, Arg9)SP and (Arg9)SP, but both α-helix and β-sheet structures were manifested for (Nle9)SP. The thermodynamic parameters of lipid binding were determined with monolayer expansion measurements and high-sensitivity titration calorimetry. The apparent binding constants for membranes containing 100% POPG (1-palmitoyl-2-oleoyl-sn-glycero-3-phosphoglycerol) were of the order of 10^3 to 10^5 M^{-1}. Binding was found to involve electrostatic attraction of the cationic peptides to the negatively charged membrane surface. Measurement of binding affinities to the NK-1 receptor and of the *in vitro* activities showed that all three peptides behaved as agonists. The fact that even the highly charged (Arg9)SP had agonistic activity provided evidence that the binding epitope at the receptor was in a hydrophilic environment. The results indicated that a membrane-mediated receptor mechanism was unlikely, but rather provided insight to suggest that the agonist approached the receptor-binding site from the aqueous phase.

Magainins are another example of positively charged amphiphatic peptides that permeabilize cell membranes and display antimicrobial activity. Magainins are known to bind to negatively and neutral charged membranes.[119] The binding properties have been characterized using ITC and are believed to occur by a surface partition equilibrium mechanism. Binding was found to proceed via large exothermic reaction enthalpies ranging from –15 to –18 kcal/mol (at 30°C). Determination of the ΔCp_b by plotting the ΔH_b as a function of temperature (i.e., in the same way illustrated in Figure 13.11) yielded a large positive value of 130 cal/mol-°K. The corresponding ΔG_b was found to be between –6.4 and –8.6 kcal/mol, resulting in a large, less favorable negative ΔS_b. Hence, the binding of magainin to small unilamellar vesicles is an enthalpy-driven reaction. Circular dichroism experiments provided further evidence that the membrane-bound fraction of magainin was approximately 80% helical at 8°C, decreasing to about 60% at 45°C. Knowing that the random coil-to-helix transition in aqueous solution is known to be exothermic, the same process occurring at the membrane surface may account for up to 65% of the measured enthalpy.[119] Hence, membrane-facilitated helix formation is followed by insertion of the nonpolar amino side chains into the lipid bilayer. In the same study it was shown that cholesterol drastically reduced the extent of magainin binding and exhibited enthalpy–entropy compensation.

The effects of pH, ionic strength, and temperature on the thermodynamics of medium-chain acyl-CoA dehydrogenase (MCAD)–octenoyl-CoA interaction have been studied.[120] The binding reaction is characterized by a stoichiometry of 0.89 mol of octenoyl-CoA/mole MCAD subunit. Thermodynamic parameters at 25°C include ΔG_b = –8.75 kcal/mol, ΔH_b = –10.3 kcal/mol, and ΔS_b = –5.3 cal/mol-°K, indicating that the formation of the complex is enthalpy-driven in a solution containing 50 m*M* phosphate buffer, pH 7.6 and ionic strength of 175 m*M*. The study showed that although ionic strength did not significantly influence the complex reaction, the pH of the buffer media had a pronounced effect. The ΔCp_b of this complex reaction was found to be –0.37 kcal/mol-°K, indicating that the binding of octenoyl-CoA to MCAD is dominated by hydrophobic forces. However, for some systems like cytochrome c interactions with negatively charged dioleoylphosphatidylglycerol (DOPG), it has been shown that the binding constant and enthalpy of association decrease with increasing ionic strength, where no binding is detected above 0.5 *M* NaCl.[121] Hence, in some cases, salt can be a powerful modulator of binding activity when electrostatics define the binding mechanism.

It is interesting that modifying solution conditions by adding different concentrations of ethanol can produce a biphasic effect on melting transition temperatures of lipid-like systems (e.g., acyl chains of hydrocarbons). For example, low concentrations of ethanol reduce the T_m of phosphatidylcholine bilayers, whereas higher concentrations increase the T_m of the same system.[122] This effect has been shown to depend upon acyl chain length and can be explained by the

fact that interdigitated phases are formed in which there is an energy gain because van der Waals energy is augmented in more closely packed phases of this type. Interdigitated phases are favored with high ethanol concentrations in which the hydrocarbon chains are more highly ordered, resulting in narrow phase transitions.

Lipid systems are of special interest to those working in the area of drug delivery. Liposomes are currently being considered as vehicles for target delivery of biologics and peptides.[123,124] In order to facilitate rational approaches in the development of novel delivery systems of this type, the properties of the liposome and the active drug need to be taken into account to better understand stabilization. Microcalorimetry has been useful in the determination of such interactions between different proteins and their interactions with various lipid systems (i.e., neutral lipid, dipalmitoylphophatidylcholine, DPPC; negatively charged lipid, dipalmitoylphosphatidylglycerol, DPPG). According to Papahajopoulos and coworkers,[125] proteins can be classified into three categories, based upon their thermotropic behavior with a given phospholipid. For example in the first category, proteins that are predominantly hydrophilic (i.e., polylysine and ribonuclease A) have been thought to absorb onto the bilayer surface by simple electrostatic interactions, exerting a stronger effect on the phase transitions of charged rather than zwitterionic phospholipids. The second category is ascribed to proteins that are partially hydrophilic and hydrophobic, able to associate on the surface via electrostatic forces, but that also may become embedded into the bilayer (i.e., cytochrome c, myelin basic protein [A-1]). Finally, the third category is characterized by proteins that can penetrate into the core of anionic or zwitterionic lipid bilayers characterized by strong hydrophobic interactions (i.e., gramicidin A and proteolipid apoprotein [N-2]). More recent investigation of this scheme of classification has revealed that hydrophilic proteins do not bind to liposomes exclusively at the surface by electrostatic interactions, and some degree of penetration is observed in most cases.[124] Moreover, superoxide dismutase was found to unexpectedly bind DPPG and, as a result, was thought to protect lipid membranes against oxygen-mediated injury.

Recombinant human granulocyte colony-stimulating factor (rhG-CSF) interacts with liposomes composed of the anionic phospholipid DOPG, and this interaction enhances the stability of the protein.[126] Recombinant hG-CSF inserts into bilayers of anionic, but not zwitterionic phospholipids, making this system conform to category 2 of the Papahajopoulos scheme. Isothermal titration analysis of this protein with dimyristoylphosphatidylglycerol (DMPG) at 25°C indicated that the binding was saturable, involving 10 lipids/rhG-CSF.[127] This titration experiment is endothermic, having a $Ka = 4.3 \times 10^5\ M^{-1}$, $\Delta H_b = 5.42$ kcal/mol, $\Delta G_b = -7.69$ kcal/mol, and a $\Delta S_b = 44$ cal/mol-°K. The large favorable ΔS_b indicates that this reaction is entropically driven. In the same study it was shown that the stabilization of rhG-CSF by anionic phospholipids required a chain length that was $\geq C_{10}$. Moreover, the stabilization of other growth factors that were structurally similar to rhG-CSF (i.e., recombinant porcine somatotropin, recombinant human interleukin 4, recombinant human interleukin 2, recombinant human

granulocyte-macrophage CSF) were stabilized by the anionic phospholipid DMPG. This study showed that a group of structurally similar proteins can interact preferentially with anionic phospholipids and that the complexation of the growth factors with vesicles composed of anionic phospholipids improves the stability of the proteins under conditions where they normally denature.

The nature of lipid structure variation and its influence on the stability of integral membrane proteins has been investigated by microcalorimetry. For example, in the structural stability of erythrocyte anion transporter, band 3 has been studied in different lipid environments.[125] This protein system falls into the third category defined by Papahajopoulos and coworkers. The data revealed that the stability of the 55-kDa membrane-spanning domain of band 3 was exquisitely sensitive to the acyl chain length of its phospholipid environment, increasing almost linearly from a T_m of 47°C in DPPC (C14:1) to 66°C in dinervonylphosphatidylcholine (C24:1). It was shown that although band 3 was native in all reconstituted lipid systems, the transport protein's stability was found to be much greater in zwitterionic lipids (i.e., phosphatidylethanolamine, phosphatidylcholine). In a subsequent study of this system, fatty acids that most effectively stabilized band 3 also yielded the highest affinity for the transporter protein.[128]

PRESSURE PERTURBATION CALORIMETRY (PPC)

The PPC method is a relatively new technique that is based upon the measurement of volumetric properties of proteins in dilute solutions. This technique, developed by MicroCal, LLC (Northampton, MA), measures the heat change (ΔQ) that results from a change in pressure (ΔP) above a solution containing dissolved protein. The total fill volume of the sample (containing the protein analyte) and reference (identical buffer solution) cells have identical volumes of 0.5 ml. The experimental design involves access of both cells to a common pressure chamber (containing a pressure sensor that transmits data to the computer). Pressure in the chamber alternates between P1 and P2 (Figure 13.12), operating at selected pressures ranging from 0 to 5 atm. The calorimetric baseline is first allowed to equilibrate before a pressure P1 is applied. The excess pressure is then changed to P2, causing heat to be absorbed in both cells. Because the solutions in the sample and reference cells are identical except for the small amount of dissolved protein in the sample cell, counterbalanced by the corresponding volume of buffer in the reference cell, differential heats are quite small. The resulting peaks of compression and decompression are of identical size but of opposite sign. Integration of each peak provides the heat change between the reference and sample cells. Experiments can be carried out via computer control to automatically obtain data at numerous temperatures. It can be shown that ΔQ is a function of the coefficient of thermal expansion, α.[129]

What is obtained by performing such experiments across an appropriate temperature range is the precise measurement of the coefficient of thermal expansion for protein partial specific volumes that may be detected at concentrations

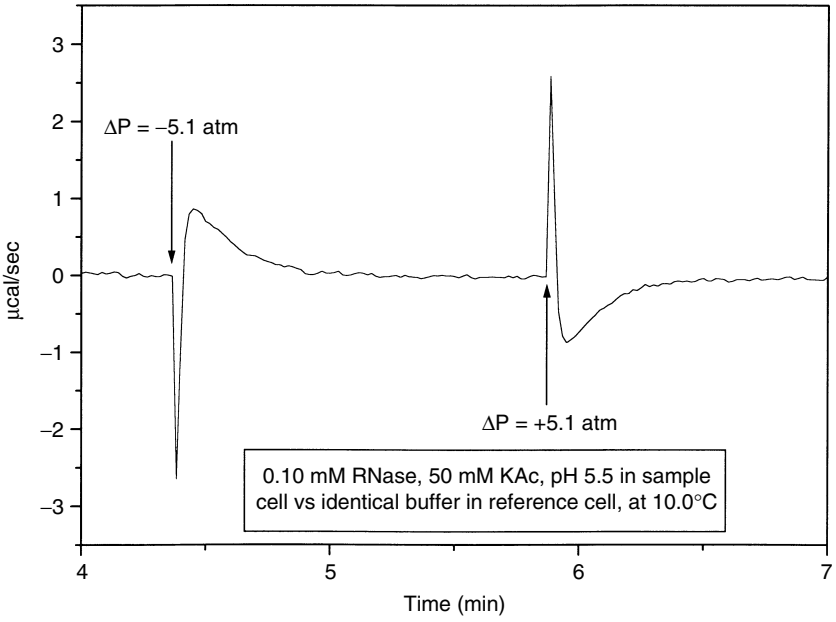

Figure 13.12 Pressure perturbation calorimetry (PPC) experiment showing alternating pressure pulses of 5.1 and +5.1 atm as a function of time. The reaction mixture comprises 0.10 m*M* RNase A, 50 m*M* potassium acetate (pH 5.5) in the sample cell with identical buffer in the reference cell. The experiment is carried out at 10°C. (Permission to use the figure granted by MicroCal, LLC.)

as low as 0.25%. The partial specific volume of a protein in solution is equal to the sum of the intrinsic volume of the protein plus the change in the volume of solvent resulting from its interaction with the accessible protein side chains. Solutes that favor an increase in water structure are expected to have a small positive (or even negative) α at low temperature with a correspondingly large positive coefficient as the temperature is raised.[130] The converse is true for solutes that decrease water structure (i.e., hydrophilic and salt compounds). The nature of the solvation contribution to α can therefore be assessed for a given class of amino acids using this technique. For example, the aliphatic side chains, alanine, valine, and isoleucine, are similar in that their values are negative at low temperature, with a strong positive slope and negative curvature as temperature increases (Figure 13.13). Because water tends to be arranged in an orderly fashion around apolar surfaces (as already mentioned, this is accommodated by a decrease in entropy), such side chains may be considered "structure makers." In contrast, aromatic side chains like tryptophan and phenylalanine are positive and nearly independent of temperature. By comparison, polar side chains such as asparagine,

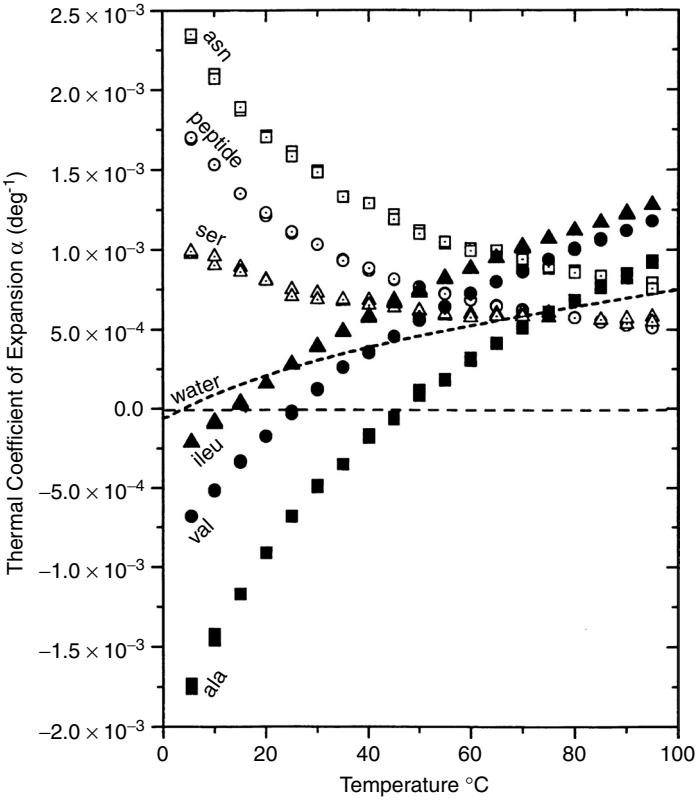

Figure 13.13 A plot showing the behavior of the thermal coefficient of expansion α (deg^{-1}) for different amino acids, peptide, and water as a function of temperature measured by PPC. The dashed curve displays the estimated progress baseline for the pre- and posttransition region. (Permission to use the figure granted by MicroCal, LLC.)

serine, and other highly polar peptide groups exhibit highly positive values at low temperature with a characteristic negative slope and positive curvature with increasing temperature (Figure 13.13). Such behavior is consistent with the "structure-breaking" properties of solvated water in these cases, given the tendency for water to adopt a more disordered structure (entropy is favored). This is also the case with other hydrophilic side chains and various electrolytes.

Globular proteins typically have their hydrophobic side chains buried to remove them from the polar water solvent. Hence, a proportionately greater hydrophilic surface is in contact with the solvent at a given instant. Proteins like ribonuclease A and chymotrypsinogen exhibit decreasing α values with increasing temperature that is consistent with "structure breakers" (Figure 13.14). Generally,

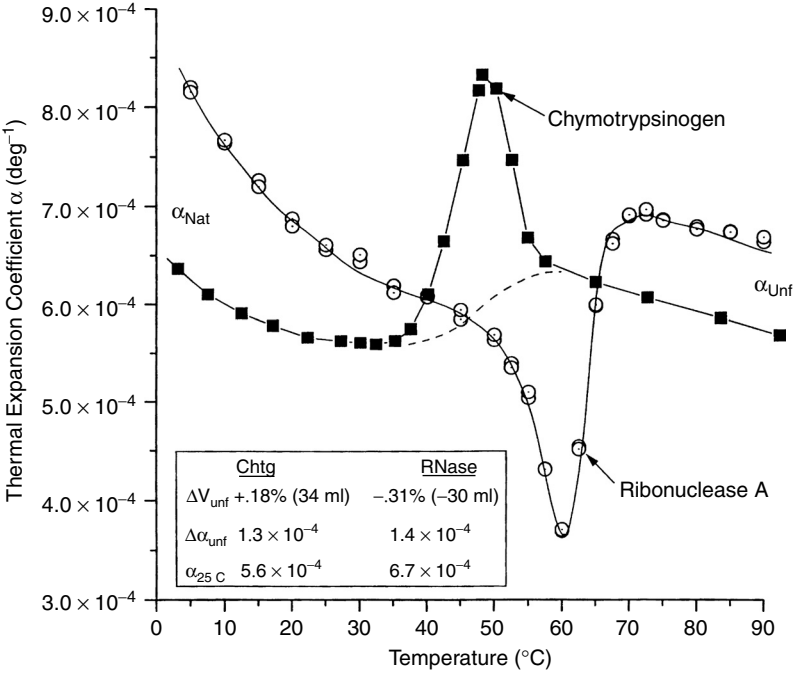

Figure 13.14 The PPC traces of the thermal expansion coefficient α (deg^{-1}) as a function of temperature for chymotrypsinogen and RNase A. The data show that both native (low-temperature region) proteins exhibit a strong negative temperature coefficient as well as a large positive curvature. (Permission to use the figure granted by MicroCal, LLC.)

when the protein unfolds at high temperature, the solvent-accessible surface area (ASA) will increase and so will α (as in the case of chymotrypsinogen). Computational studies have been performed on the mutant stability of T4 lysozyme, and they correlate with the surface thermal expansion of the protein.[131] In contrast to the positive change in the volume of unfolding (ΔV_{unf}, obtained by integrating over the temperature range where the transition occurs) concerning chymotrypsinogen, ribonuclease A exhibits a negative change in unfolding volume (Figure 13.14). The correlation of such data may one day lead to the ability to predict the stability outcome of a given engineered biologic based upon its thermal expansion properties within a given formulation environment. Alternatively, it might be possible to use such information to modify specific amino acid sites that confer greater stability in a given biologic. The combination of PPC data with improved computational approaches could facilitate a more detailed understanding about the effects of thermal behavior and the prediction of protein stability in different solution environments.

CHALLENGES

Thermodynamic–Kinetic Relationships

The study of reaction rates or kinetics of a particular denaturation process of a protein therapeutic can provide valuable information about the mechanism, i.e., the sequence of steps that occur in the transformation of the protein to chemically or conformationally denatured products. The kinetics tell something about the manner in which the rate is influenced by such factors as concentration, temperature, excipients, and the nature of the solvent as it pertains to properties of protein stability. The principal application of this information in the biopharmaceutical setting is to predict how long a given biologic will remain adequately stable.

Applying kinetics to denaturation studies must take into account the thermodynamic properties associated with the energetics of the reaction process. Thermodynamic properties are ascribed to the equilibrium between the native and the denatured states. For example, M-2 glycoprotein does not bind thyroxine in its native state, but when heat denatured, acquires thyroxine-binding properties with an associated ΔH_b of 1.5 kcal/mol.[132] Likewise, the reaction rate will be affected by the proportion and extent of thermally unfolded forms that may participate in the binding reaction. The concept that protein conformational changes are related to the energetics and mechanism of reactions was suggested by Rufus Lumry and Henry Eyring in 1954.[133] They reasoned that because the native state could be perturbed by any large change in solvent composition, temperature, or pressure producing alterations attributed to conformational isomers that made up a denatured ensemble (of relatively higher energy states), complex kinetics would ensue. Therefore, a reaction originating from an altered or more unfolded conformation would in fact emanate not just from one major species, but from many. Reaction paths of lower free energy would be available for selected conformations with emphasis on the participation of one or a few forms. The overall reaction, however, would be the sum of the processes that originated from the native state (or a number of closely related states) and end at another group of closely related states. This situation could be taken into account by summing the rate of reactant loss, $-dR_i/dt$, over all reaction paths i and thus over all activated complexes of concentration C_i^*. They had noted that Arrhenius plots of protein "transconformation" and enzymatic reactions were frequently nonlinear, as expected when several simultaneous processes produced the same product. They surmised that this resulted from different activation energies or a changing distribution of species with temperature, and concluded that the kinetic products formed from heat-denatured protein must depend on the speed of the initial reaction, no matter whether the intermediate product formed in equilibrium or as a steady-state intermediate.

Arrhenius plots permit the determination of activation energies (Ea) associated with a particular pathway of degradation that allows one to estimate reaction rates as a function of temperature. Such information, if demonstrated to accurately model

the reaction, can make it possible to predict longevity of biopharmaceutical products stored at real-time conditions. To be useful, it is important to factor in the consequences of protein unfolding as it affects *Ea*. In fact, there is evidence of change in reaction rates at different temperatures and different amounts of unfolding. An example is described by the unusual temperature dependence of ovalbumin at the first stage of urea denaturation.[134,135] At low temperature, the rate constant decreases sharply as temperature increases with an apparent *Ea* of about –28 kcal/mol at 0°C. Near 20°C, the rate constant becomes independent of temperature so that *Ea* is zero. Finally, at higher temperatures the rate constant increases with temperature and *Ea* approaches 50 kcal/mol. In the absence of urea the *Ea* is 130 kcal/mol. In another example, IL-1R (type II) aggregation has been recently shown to exhibit two different activation energies across a temperature regime spanning from 30 to 75°C. What was interesting about the discontinuity in the two activation energies was that it happened to occur in the vicinity of the T_m for this molecule.[136] This latter result provided compelling evidence that the aggregation pathway depended on the unfolding of the IL-1R (II) molecule.

Microcalorimetry can be used to determine activation energies of denaturation reactions. In general, scan rates of 60°C/h are considered to be adequate for simple, reversible unfolding transitions in which the melting transition should be unaffected by different scan rates.[137] However, in some cases, kinetically controlled irreversible processes can occur (i.e., aggregation, or chemical degradation at elevated temperatures) that can affect the onset slope of the endotherm describing the reaction, causing the T_m to shift in a scan rate-dependent manner. In such situations, a change in the apparent T_m behavior (because the true melting temperature in this instance is not precisely known) as a function of different scan rates using a modified form of the Arrhenius equation can permit determination of the *Ea* of the reaction.[138] A plot of ln (v/T_m^2) as a function of 1/T results in a straight line with slope of *Ea*/R (where v is the scan rate in units of °K/min). The validity of this approach to determining activation energies has been demonstrated for the thermal denaturation of thermolysin[138] and carboxypeptidase B.[139] In both cases this treatment was applied to systems that were shown to be completely irreversible. An example of such a plot for the case of thermolysin is illustrated in Figure 13.15. A tri-state model was used to describe the experimental behavior, shown by the scheme below.

$$N \underset{k_{-1}}{\overset{k_1}{\rightleftharpoons}} D \xrightarrow{k_2} D_I$$

Here, in association with the dynamics of the native (N) to denatured (unfolded, D) state, there are associated rate constants for the forward and reverse reactions. In some cases of thermal denaturation, the forward reaction rate denoted by k_1 is much greater than the reverse reaction (k_{-1}) associated with refolding and $k_2 \gg k_1$.[138–140] When this is true (i.e., completely irreversible process), the scheme above may be reduced to the following:

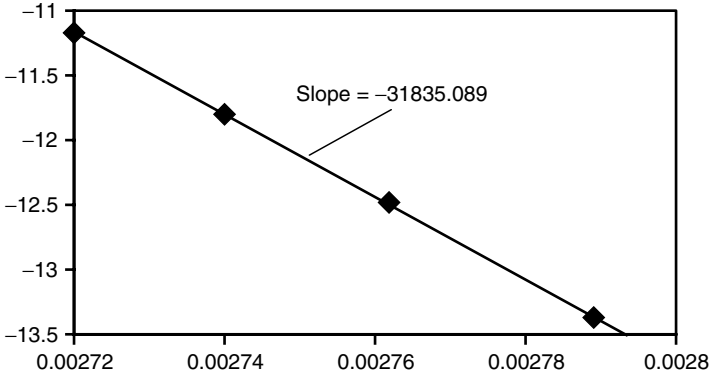

Figure 13.15 A plot of ln (v/T_m^2) vs. $1/T_m$ for the thermal denaturation of thermolysin using DSC scan rates of 1.9, 1.0, 0.5, and 0.2 °K/min. The plot assumes Arrhenius behavior holds. The slope of the plot is equal to $-Ea/R$. Using R = 1.9872 cal/deg-mol, one can calculate the activation energy to be ~ 63.3 kcal/mol. (Data plotted were obtained from Reference 138.)

$$N \xrightarrow{k'} D_I$$

In this approach, the rate of the reaction is kinetically controlled and k′ is the rate constant for the formation of the irreversibly denatured product, D_I.

It should be noted that the unfolding kinetics can sometimes involve quite complex unfolding schemes of different substates in equilibrium with the native state. Staphylococcal nuclease is an example of such behavior, known to unfold with three different substates that exhibit an equilibrium that does not appear to shift with temperature.[49] Irreversible aggregation processes of proteins have been known to involve first- or second-order reactions.[132,141] The mechanism of recombinant human interferon-γ aggregation is an example where thermodynamic and kinetic aspects of the reaction provided a powerful tool for understanding the pathway of instability and permitted a rationale for screening excipients that inhibited the process.[141]

The stability of a biological is a key aspect of quality, and regulatory authorities recognize that useful-life claims need to be realistic and demonstrable. A shelf-life is tentatively assigned on the basis of accelerated stability data. When predicting a shelf-life from accelerated storage conditions, a reaction order is determined with an associated rate constant and activation energy. This information may then be used to predict the rate of decomposition at low temperatures where the biopharmaceutical is to be stored in real time.[142] Arrhenius kinetics have been applied to other forms of instability with some success toward predicting shelf-life, e.g., the chemical decomposition of human epidermal growth factor (hEGF) by oxidation, deamidation, and succinimide processes.[89] Arrhenius plots of

the apparent first-order rates yielded respectable activation energies that correlated well with observed shelf-life expectancy predictions at lower temperatures.

The application to predicting shelf-life based upon Arrhenius modeling is fraught with challenges. All of the complexities of the reaction, whether it involves intermediates of unfolding (i.e., multidomain protein systems), chemical modifications of the protein, or proteolysis, can affect reaction rates differently with respect to temperature. Hence, in order to be accurate, a detailed account of each destabilizing influence, along with its dependence on conformation, should be considered as a function of temperature. Rates of different reactions or mechanisms, although exhibiting Arrhenius behavior, may be compensatory with temperature. That is, some reaction rates slow down with temperature, whereas others increase, compensating for the overall rate of the denaturation reaction. Where conformation plays a role in the amount and type of degradation products formed, attention should be given to ascertaining the degree of unfolding acquired at low-temperature conditions. Sometimes very little unfolding is required to propagate an aggregation product.[49–51,141,143] In the case of proteins composed of several cooperative unfolding domains, it may be necessary to characterize the influence of each domain as it contributes to the overall reaction process.

There are four underlying assumptions regarding Arrhenius kinetics. First, that the concentration dependence (assignable to the order of the reaction) associated with the kinetics of the reaction can be described in terms of a single mechanism of instability (i.e., aggregation, hydrolysis, proteolysis, deamidation) without influence of competing reactions. Second, that the predominant mechanisms at elevated temperatures are the same at lower temperatures. Third, reaction by-products have little influence on the reaction rate. Fourth, accurate control of the temperature is achieved. Regarding this point, the determination of *Ea* using microcalorimetry has an advantage over conventional reaction studies with incubators, or temperature baths, because of the greater insulation and lower temperature flux associated with such instruments. Finally, it is assumed that solution conditions remain constant for the duration of the experiment (i.e., pH, ionic strength) and correctly represent kinetic behavior at accelerated conditions. The best way to understand the role of the underlying assumptions is to carry out kinetic studies at several accelerated temperature conditions (being mindful of the T_m) and compare the rates to those stored at real-time conditions (using *Ea* to estimate performance). It is anticipated that microcalorimetry will play an integral role in the accumulation of such data, providing knowledge of the predominant mechanisms involved and adding significance to the Arrhenius models used for making shelf-life predictions acceptable. Implied in this endeavor is the development of good stability-indicating assays that can support and quantitatively characterize protein reactions of instability.

High-Throughput Methodologies

Another area of development that could greatly improve the ability to rapidly derive stable liquid formulation candidates is the development of high-throughput

microcalorimetry instruments. As already mentioned, this has been a limitation that does not lend itself to screening multiple excipients in an efficient manner. The availability of such instruments will make it possible to not only determine which excipients to include in a given formulation, but can also be used to determine optimization of excipient concentrations as they affect stability. This challenge has been undertaken by MicroCal, LLC, where a high-throughput capillary-DSC instrument has been developed with the capability of performing up to 50 scans during 24 h of unattended operation. Automated instruments of this kind are now readily available.

References

1. Jiang, X., J. Kowalski, and J.W. Kelly. 2001. Increasing protein stability using a rational approach combining sequence homology and structural alignment: stabilizing the WW domain. *Protein Sci* 10: 1454–1465.
2. van Gunsteren, W.F. and A.E. Mark. 1992. Prediction of the activity and stability effects of site-directed mutagenesis on a protein core. *J Mol Biol* 227: 389–395.
3. Bartolucci, S., A. Guagliardi, E. Pedone, D. De Pascale, R. Cannio, L. Camardella, M. Rossi, G. Nicastro, C. de Chiara, P. Facci, G. Mascetti, and C. Nicolini. 1997. Thioredoxin from *Bacillus acidocaldarius*: characterization, high-level expression in *Escherichia coli* and molecular modelling. *Biochem J* 328: 277–285.
4. Bombardier, H., P. Wong, and C. Gicquaud. 1997. Effects of nucleotides on the denaturation of F actin: a differential scanning calorimetry and FTIR spectroscopy study. *Biochem Biophys Res Commun* 236: 798–803.
5. Boye, J.I., A.A. Ismail, and I. Alli. 1996. Effects of physicochemical factors on the secondary structure of beta-lactoglobulin. *J Dairy Res* 63: 97–109.
6. Brass, O., J.M. Letoffe, A. Bakkali, J.C. Bureau, C. Corot, and P. Claudy. 1995. Involvement of protein solvation in the interaction between a contrast medium (iopamidol) and fibrinogen or lysozyme. *Biophys Chem* 54: 83–94.
7. Waldner, J.C., S.J. Lahr, M.H. Edgell, and G.J. Pielak. 1999. Nonideality and protein thermal denaturation. *Biopolymers* 49: 471–479.
8. Welfle, K., R. Misselwitz, G. Hausdorf, W. Hohne, and H. Welfle. 1999. Conformation, pH-induced conformational changes, and thermal unfolding of anti-p24 (HIV-1) monoclonal antibody CB4-1 and its Fab and Fc fragments. *Biochim Biophys Acta* 1431: 120–131.
9. Zaiss, K. and R. Jaenicke. 1999. Thermodynamic study of phosphoglycerate kinase from *Thermotoga maritima* and its isolated domains: reversible thermal unfolding monitored by differential scanning calorimetry and circular dichroism spectroscopy. *Biochemistry* 38: 4633–4639.
10. Chen, B.L., T. Arakawa, C.F. Morris, W.C. Kenney, C.M. Wells, and C.G. Pitt. 1994. Aggregation pathway of recombinant human keratinocyte growth factor and its stabilization. *Pharm Res* 11: 1581–1587.
11. De Young, L.R., K.A. Dill, and A.L. Fink. 1993. Aggregation and denaturation of apomyoglobin in aqueous urea solutions. *Biochemistry* 32: 3877–3886.
12. Mitraki, A., J.M. Betton, M. Desmadril, and J.M. Yon. 1987. Quasi-irreversibility in the unfolding-refolding transition of phosphoglycerate kinase induced by guanidine hydrochloride. *Eur J Biochem* 163: 29–34.

13. Powell, M.F. 1994. In *Formulation and Delivery of Proteins and Peptides*. J.L. Cleland and R. Langer, editors. American Chemical Society, Washington, D.C., 100–117.
14. Remmele, R.L., Jr. and W.R. Gombotz. 2000. Differential scanning calorimetry: a practical tool for elucidating stability of liquid biopharmaceuticals. *Biopharm* 13: 36–46.
15. Wearne, S.J. and T.E. Creighton. 1989. Effect of protein conformation on rate of deamidation: ribonuclease A. *Proteins* 5: 8–12.
16. Plotnikov, V.V., J.M. Brandts, L.N. Lin, and J.F. Brandts. 1997. A new ultrasensitive scanning calorimeter. *Anal Biochem* 250: 237–244.
17. Brandts, J.F. 1967. Heat effects on proteins and enzymes. In *Thermobiology*. A.H. Rose, editor. Academic Press, New York, 25–75.
18. Pace, C.N., B.A. Shirley, M. McNutt, and K. Gajiwala. 1996. Forces contributing to the conformational stability of proteins. *Faseb J* 10: 75–83.
19. Tanford, C. 1973. In *The Hydrophobic Effect: Formation of Micelles and Biological Membranes*. John Wiley & Sons, New York.
20. Kauzmann, W. 1959. Some factors in the interpretation of protein denaturation. *Adv Protein Chem* 14: 1–64.
21. Privalov, P.L. and S.J. Gill. 1988. Stability of protein structure and hydrophobic interaction. *Adv Protein Chem* 39: 191–234.
22. Sturtevant, J.M. 1987. Biochemical applications of differential scanning calorimetry. *Ann Rev Phys Chem* 38: 463–488.
23. Chan, H.K., K.L. Au-Yeung, and I. Gonda. 1996. Effects of additives on heat denaturation of rhDNase in solutions. *Pharm Res* 13: 756–761.
24. Chang, B.S., C.S. Randall, and Y.S. Lee. 1993. Stabilization of lyophilized porcine pancreatic elastase. *Pharm Res* 10: 1478–1483.
25. Lee, L.L. and J.C. Lee. 1987. Thermal stability of proteins in the presence of poly(ethylene glycols). *Biochemistry* 26: 7813–7819.
26. Liggins, J.R., F. Sherman, A.J. Mathews, and B.T. Nall. 1994. Differential scanning calorimetric study of the thermal unfolding transitions of yeast iso-1 and iso-2 cytochromes c and three composite isozymes. *Biochemistry* 33: 9209–9219.
27. Maneri, L.R. and P.S. Low. 1988. Structural stability of the erythrocyte anion transporter, band 3, in different lipid environments. A differential scanning calorimetric study. *J Biol Chem* 263: 16170–16178.
28. Davio, S.R., K.M. Kienle, and B.E. Collins. 1995. Interdomain interactions in the chimeric protein toxin sCD4(178)-PE40: a differential scanning calorimetry (DSC) study. *Pharm Res* 12: 642–648.
29. Martinez, J.C., M. el Harrous, V.V. Filimonov, P.L. Mateo, and A.R. Fersht. 1994. A calorimetric study of the thermal stability of barnase and its interaction with 3′GMP. *Biochemistry* 33: 3919–3926.
30. North, M.J. 1993. Prevention of unwanted proteolysis. In *Proteolytic Enzymes: a Practical Approach*. R.J. Beynon and J.S. Bond, editors. IRL Press, Oxford,
31. Remmele, R.L., Jr., N.S. Nightlinger, S. Srinivasan, and W.R. Gombotz. 1998. Interleukin-1 receptor (IL-1R) liquid formulation development using differential scanning calorimetry. *Pharm Res* 15: 200–208.
32. Schrier, J.A., R.A. Kenley, R. Williams, R.J. Corcoran, Y. Kim, R.P. Northey, Jr., D. D'Augusta, and M. Huberty. 1993. Degradation pathways for recombinant human macrophage colony-stimulating factor in aqueous solution. *Pharm Res* 10: 933–944.

33. Beldarrain, A., J.L. Lopez-Lacomba, G. Furrazola, D. Barberia, and M. Cortijo. 1999. Thermal denaturation of human gamma-interferon. A calorimetric and spectroscopic study. *Biochemistry* 38: 7865–7873.
34. Blaber, S.I., J.F. Culajay, A. Khurana, and M. Blaber. 1999. Reversible thermal denaturation of human FGF-1 induced by low concentrations of guanidine hydrochloride. *Biophys J* 77: 470–477.
35. Christensen, T., B. Svensson, and B.W. Sigurskjold. 1999. Thermodynamics of reversible and irreversible unfolding and domain interactions of glucoamylase from *Aspergillus niger* studied by differential scanning and isothermal titration calorimetry. *Biochemistry* 38: 6300–6310.
36. Medved, L.V., M. Migliorini, I. Mikhailenko, L.G. Barrientos, M. Llinas, and D.K. Strickland. 1999. Domain organization of the 39-kDa receptor-associated protein. *J Biol Chem* 274: 717–727.
37. Sturtevant, J.M. 1980. Differential scanning calorimetry: processes involving proteins. In *Bioenergetics and Thermodynamics: Model Systems*. A. Braibanti, editor. John Wiley & Sons, New York, 391–396.
38. Privalov, P.L., N.N. Khechinashvili, and B.P. Atanasov. 1971. Thermodynamic analysis of thermal transitions in globular proteins. I. Calorimetric study of chymotrypsinogen, ribonuclease and myoglobin. *Biopolymers* 10: 1865–1890.
39. Privalov, P.L. 1979. Stability of proteins: small globular proteins. *Adv Protein Chem* 33: 167–241.
40. Hu, C.Q. and J.M. Sturtevant. 1987. Thermodynamic study of yeast phosphoglycerate kinase. *Biochemistry* 26: 178–182.
41. Morris, A.E., R.L. Remmele, Jr., R. Klinke, B.M. Macduff, W.C. Fanslow, and R.J. Armitage. 1999. Incorporation of an isoleucine zipper motif enhances the biological activity of soluble CD40L (CD154). *J Biol Chem* 274: 418–423.
42. Steadman, B.L., P.A. Trautman, E.Q. Lawson, M.J. Raymond, D.A. Mood, J.A. Thomson, and C.R. Middaugh. 1989. A differential scanning calorimetric study of the bovine lens crystallins. *Biochemistry* 28: 9653–9658.
43. Lepock, J.R., K.P. Ritchie, M.C. Kolios, A.M. Rodahl, K.A. Heinz, and J. Kruuv. 1992. Influence of transition rates and scan rate on kinetic simulations of differential scanning calorimetry profiles of reversible and irreversible protein denaturation. *Biochemistry* 31: 12706–12712.
44. Vogl, T., C. Jatzke, H.J. Hinz, J. Benz, and R. Huber. 1997. Thermodynamic stability of annexin V E17G: equilibrium parameters from an irreversible unfolding reaction. *Biochemistry* 36: 1657–1668.
45. Livingstone, J.R., R.S. Spolar, and M.T. Record, Jr. 1991. Contribution to the thermodynamics of protein folding from the reduction in water-accessible nonpolar surface area. *Biochemistry* 30: 4237–4244.
46. Kholodenko, V. and E. Freire. 1999. A simple method to measure the absolute heat capacity of proteins. *Anal Biochem* 270: 336–338.
47. Ganesh, C., N. Eswar, S. Srivastava, C. Ramakrishnan, and R. Varadarajan. 1999. Prediction of the maximal stability temperature of monomeric globular proteins solely from amino acid sequence. *FEBS Lett* 454: 31–36.
48. Privalov, P.L. and N.N. Khechinashvili. 1974. A thermodynamic approach to the problem of stabilization of globular protein structure: a calorimetric study. *J Mol Biol* 86: 665–684.

49. Chen, H.M., J.L. You, V.S. Markin, and T.Y. Tsong. 1991. Kinetic analysis of the acid and the alkaline unfolded states of staphylococcal nuclease. *J Mol Biol* 220: 771–778.
50. Shortle, D. 1996. The denatured state (the other half of the folding equation) and its role in protein stability. *Faseb J* 10: 27–34.
51. Uversky, V.N., A.S. Karnoup, D.J. Segel, S. Seshadri, S. Doniach, and A.L. Fink. 1998. Anion-induced folding of Staphylococcal nuclease: characterization of multiple equilibrium partially folded intermediates. *J Mol Biol* 278: 879–894.
52. Privalov, P.L. and S.A. Potekhin. 1986. Scanning microcalorimetry in studying temperature-induced changes in proteins. *Methods Enzymol* 131: 4–51.
53. Jelesarov, I. and H.R. Bosshard. 1999. Isothermal titration calorimetry and differential scanning calorimetry as complementary tools to investigate the energetics of biomolecular recognition. *J Mol Recognit* 12: 3–18.
54. Remmele, R.L., Jr., S.D. Bhat, D.H. Phan, and W.R. Gombotz. 1999. Minimization of recombinant human Flt3 ligand aggregation at the T_m plateau: a matter of thermal reversibility. *Biochemistry* 38: 5241–5247.
55. Narhi, L.O., J.S. Philo, B. Sun, B.S. Chang, and T. Arakawa. 1999. Reversibility of heat-induced denaturation of the recombinant human megakaryocyte growth and development factor. *Pharm Res* 16: 799–807.
56. Chen, B.L. and T. Arakawa. 1996. Stabilization of recombinant human keratinocyte growth factor by osmolytes and salts. *J Pharm Sci* 85: 419–426.
57. Lee, J.C. and S.N. Timasheff. 1981. The stabilization of proteins by sucrose. *J Biol Chem* 256: 7193–7201.
58. Sola-Penna, M., A. Ferreira-Pereira, A.P. Lemos, and J.R. Meyer-Fernandes. 1997. Carbohydrate protection of enzyme structure and function against guanidinium chloride treatment depends on the nature of carbohydrate and enzyme. *Eur J Biochem* 248: 24–29.
59. Lam, X.M., T.W. Patapoff, and T.H. Nguyen. 1997. The effect of benzyl alcohol on recombinant human interferon-gamma. *Pharm Res* 14: 725–729.
60. Kolvenbach, C.G., L.O. Narhi, J.S. Philo, T. Li, M. Zhang, and T. Arakawa. 1997. Granulocyte-colony stimulating factor maintains a thermally stable, compact, partially folded structure at pH2. *J Pept Res* 50: 310–318.
61. Makarov, A.A., I.I. Protasevich, E.G. Frank, I.B. Grishina, I.A. Bolotina, and N.G. Esipova. 1991. The number of cooperative regions (energetic domains) in a pepsin molecule depends on the pH of the medium. *Biochim Biophys Acta* 1078: 283–288.
62. Makarov, A.A., I.I. Protasevich, N.P. Bazhulina, and N.G. Esipova. 1995. Heat denaturation of pepsinogen in a water-ethanol mixture. *FEBS Lett* 357: 58–61.
63. Lee, J.C. 2000. Biopharmaceutical formulation. *Curr Opin Biotechnol* 11: 81–84.
64. Poklar, N., N. Petrovcic, M. Oblak, and G. Vesnaver. 1999. Thermodynamic stability of ribonuclease A in alkylurea solutions and preferential solvation changes accompanying its thermal denaturation: a calorimetric and spectroscopic study. *Protein Sci* 8: 832–840.
65. Bam, N.B., J.L. Cleland, J. Yang, M.C. Manning, J.F. Carpenter, R.F. Kelley, and T.W. Randolph. 1998. Tween protects recombinant human growth hormone against agitation-induced damage via hydrophobic interactions. *J Pharm Sci* 87: 1554–1559.
66. Baudys, M., T. Uchio, D. Mix, D. Wilson, and S.W. Kim. 1995. Physical stabilization of insulin by glycosylation. *J Pharm Sci* 84: 28–33.

67. Yan, B., W. Zhang, J. Ding, and P. Gao. 1999. Sequence pattern for the occurrence of N-glycosylation in proteins. *J Protein Chem* 18: 511–521.
68. Ghirlando, R., J. Lund, M. Goodall, and R. Jefferis. 1999. Glycosylation of human IgG-Fc: influences on structure revealed by differential scanning micro-calorimetry. *Immunol Lett* 68: 47–52.
69. Tischenko, V.M., V.M. Abramov, and V.P. Zav'yalov. 1998. Investigation of the cooperative structure of Fc fragments from myeloma immunoglobulin G. *Biochemistry* 37: 5576–5581.
70. Wang, C., M. Eufemi, C. Turano, and A. Giartosio. 1996. Influence of the carbohydrate moiety on the stability of glycoproteins. *Biochemistry* 35: 7299–7307.
71. Norde, W. and C.A. Haynes. 1995. Reversibility and the mechanism of protein adsorption. In *Proteins at Interfaces II: Fundamentals and Applications*. T.A. Horbett and J.L. Brash, editors. American Chemical Society, Washington, D.C., 26–40.
72. Volkin, D.B., A.M. Verticelli, M.W. Bruner, K.E. Marfia, P.K. Tsai, M.K. Sardana, and C.R. Middaugh. 1995. Deamidation of polyanion-stabilized acidic fibroblast growth factor. *J Pharm Sci* 84: 7–11.
73. Williams, R.M., C.J. Brown, T. Soule, J.A. Foster, and A.K. Dunker. 2001. A scale of amino acid propensities for ordered and disordered structure. *Protein Sci* 10: 171–172.
74. Wrabl, J.O., S.A. Larson, and V.J. Hilser. 2001. Thermodynamic propensities of amino acids in the native state ensemble: implications for fold recognition. *Protein Sci* 10: 1032–1045.
75. Hilser, V.J. and E. Freire. 1996. Structure-based calculation of the equilibrium folding pathway of proteins. Correlation with hydrogen exchange protection factors. *J Mol Biol* 262: 756–772.
76. Reva, B. and S. Topiol. 2000. Recognition of protein structure: determining the relative energetic contributions of β-strands, α-helices and loops. *Pac Symp Biocomput* 5: 165–175.
77. Makhatadze, G.I., G.M. Clore, A.M. Gronenborn, and P.L. Privalov. 1994. Thermodynamics of unfolding of the all beta-sheet protein interleukin-1 beta. *Biochemistry* 33: 9327–9332.
78. Taylor, J.W., N.J. Greenfield, B. Wu, and P.L. Privalov. 1999. A calorimetric study of the folding-unfolding of an alpha-helix with covalently closed N- and C-terminal loops. *J Mol Biol* 291: 965–976.
79. Gursky, O. and D. Atkinson. 1996. High- and low-temperature unfolding of human high-density apolipoprotein A-2. *Protein Sci* 5: 1874–1882.
80. O'Brien, R., J.M. Sturtevant, J. Wrabl, M.E. Holtzer, and A. Holtzer. 1996. A scanning calorimetric study of unfolding equilibria in homodimeric chicken gizzard tropomyosins. *Biophys J* 70: 2403–2407.
81. Yu, Y., O.D. Monera, R.S. Hodges, and P.L. Privalov. 1996. Investigation of electrostatic interactions in two-stranded coiled-coils through residue shuffling. *Biophys Chem* 59: 299–314.
82. Munson, M., S. Balasubramanian, K.G. Fleming, A.D. Nagi, R. O'Brien, J.M. Sturtevant, and L. Regan. 1996. What makes a protein a protein? Hydrophobic core designs that specify stability and structural properties. *Protein Sci* 5: 1584–1593.
83. Barlow, D.J. and P.L. Poole. 1987. The hydration of protein secondary structures. *FEBS Lett* 213: 423–427.

84. Chan, M.K., S. Mukund, A. Kletzin, M.W. Adams, and D.C. Rees. 1995. Structure of a hyperthermophilic tungstopterin enzyme, aldehyde ferredoxin oxidoreductase. *Science* 267: 1463–1469.
85. Tanner, J.J., R.M. Hecht, and K.L. Krause. 1996. Determinants of enzyme thermostability observed in the molecular structure of *Thermus aquaticus* D-glyceraldehyde-3-phosphate dehydrogenase at 25 Angstroms Resolution. *Biochemistry* 35: 2597–2609.
86. Salminen, T., A. Teplyakov, J. Kankare, B.S. Cooperman, R. Lahti, and A. Goldman. 1996. An unusual route to thermostability disclosed by the comparison of *Thermus thermophilus* and *Escherichia coli* inorganic pyrophosphatases. *Protein Sci* 5: 1014–1025.
87. Liang, J. and K.A. Dill. 2001. Are proteins well-packed? *Biophys J* 81: 751–766.
88. Russell, R.J., J.M. Ferguson, D.W. Hough, M.J. Danson, and G.L. Taylor. 1997. The crystal structure of citrate synthase from the hyperthermophilic archaeon *Pyrococcus furiosus* at 1.9 Å resolution. *Biochemistry* 36: 9983–9994.
89. Senderoff, R.I., S.C. Wootton, A.M. Boctor, T.M. Chen, A.B. Giordani, T.N. Julian, and G.W. Radebaugh. 1994. Aqueous stability of human epidermal growth factor 1-48. *Pharm Res* 11: 1712–1720.
90. Senderoff, R.I., K.M. Kontor, J.K. Heffernan, H.J. Clarke, L.K. Garrison, L. Kreilgaard, G.W. Lasser, and G.B. Rosenberg. 1996. Aqueous stability of recombinant human thrombopoietin as a function of processing schemes. *J Pharm Sci* 85: 749–752.
91. Livingstone, J.R. 1996. Antibody characterization by isothermal titration calorimetry. *Nature* 384: 491–492.
92. Morton, T.A., D.B. Bennett, E.R. Appelbaum, D.M. Cusimano, K.O. Johanson, R.E. Matico, P.R. Young, M. Doyle, and I.M. Chaiken. 1994. Analysis of the interaction between human interleukin-5 and the soluble domain of its receptor using a surface plasmon resonance biosensor. *J Mol Recognit* 7: 47–55.
93. Doyle, M.L., G. Louie, P.R. Dal Monte, and T.D. Sokoloski. 1995. Tight binding affinities determined from thermodynamic linkage to protons by titration calorimetry. *Methods Enzymol* 259: 183–194.
94. Baker, B.M. and K.P. Murphy. 1996. Evaluation of linked protonation effects in protein binding reactions using isothermal titration calorimetry. *Biophys J* 71: 2049–2055.
95. Sigurskjold, B.W., C.R. Berland, and B. Svensson. 1994. Thermodynamics of inhibitor binding to the catalytic site of glucoamylase from *Aspergillus niger* determined by displacement titration calorimetry. *Biochemistry* 33: 10191–10199.
96. Sigurskjold, B.W. 2001. ITC analysis involving cubic binding equations: strong binding and self-associating ligands. Biocalorimetry 2001 Conference, Philadelphia Meeting (e-mail for a copy of algorithm: bwsigurskjold@aki.ku.dk).
97. Brandts, J.F. and L.N. Lin. 1990. Study of strong to ultratight protein interactions using differential scanning calorimetry. *Biochemistry* 29: 6927–6940.
98. Kelley, R.F., M.P. O'Connell, P. Carter, L. Presta, C. Eigenbrot, M. Covarruabias, B. Snedecor, R. Speckart, G. Blank, D. Vetterlein, and C. Kotts. 1993. Characterization of humanized anti-p185^{HER2} antibody fab fragments produced in *Escherichia coli*. *ACS Symp Ser* 526: 218–239.
99. Pearce, K.H., Jr., M.H. Ultsch, R.F. Kelley, A.M. de Vos, and J.A. Wells. 1996. Structural and mutational analysis of affinity-inert contact residues at the growth hormone-receptor interface. *Biochemistry* 35: 10300–10307.

100. Lemmon, M.A., Z. Bu, J.E. Ladbury, M. Zhou, D. Pinchasi, I. Lax, D.M. Engelman, and J. Schlessinger. 1997. Two EGF molecules contribute additively to stabilization of the EGFR dimer. *Embo J* 16: 281–294.
101. Clark, C., D. Bast, A.M. Sharp, P.M. St Hilaire, R. Agha, P.E. Stein, E.J. Toone, R.J. Read, and J.L. Brunton. 1996. Phenylalanine 30 plays an important role in receptor binding of verotoxin-1. *Mol Microbiol* 19: 891–899.
102. Gorshkova, I., J.L. Moore, K.H. McKenney, and F.P. Schwarz. 1995. Thermodynamics of cyclic nucleotide binding to the cAMP receptor protein and its T127L mutant. *J Biol Chem* 270: 21679–21683.
103. Spivak-Kroizman, T., M.A. Lemmon, I. Dikic, J.E. Ladbury, D. Pinchasi, J. Huang, M. Jaye, G. Crumley, J. Schlessinger, and I. Lax. 1994. Heparin-induced oligomerization of FGF molecules is responsible for FGF receptor dimerization, activation, and cell proliferation. *Cell* 79: 1015–1024.
104. Wu, J., J. Li, G. Li, D.G. Long, and R.M. Weis. 1996. The receptor binding site for the methyltransferase of bacterial chemotaxis is distinct from the sites of methylation. *Biochemistry* 35: 4984–4993.
105. Fields, B.A., F.A. Goldbaum, W. Dall'Acqua, E.L. Malchiodi, A. Cauerhff, F.P. Schwarz, X. Ysern, R.J. Poljak, and R.A. Mariuzza. 1996. Hydrogen bonding and solvent structure in an antigen-antibody interface. Crystal structures and thermodynamic characterization of three Fv mutants complexed with lysozyme. *Biochemistry* 35: 15494–15503.
106. Tello, D., E. Eisenstein, F.P. Schwarz, F.A. Goldbaum, B.A. Fields, R.A. Mariuzza, and R.J. Poljak. 1994. Structural and physicochemical analysis of the reaction between the anti-lysozyme antibody D1.3 and the anti-idiotopic antibodies E225 and E5.2. *J Mol Recognit* 7: 57–62.
107. Tsumoto, K., Y. Nakaoki, Y. Ueda, K. Ogasahara, K. Yutani, K. Watanabe, and I. Kumagai. 1994. Effect of the order of antibody variable regions on the expression of the single-chain HyHEL10 Fv fragment in *E. coli* and the thermodynamic analysis of its antigen-binding properties. *Biochem Biophys Res Commun* 201: 546–551.
108. Tsumoto, K., Y. Ueda, K. Maenaka, K. Watanabe, K. Ogasahara, K. Yutani, and I. Kumagai. 1994. Contribution to antibody–antigen interaction of structurally perturbed antigenic residues upon antibody binding. *J Biol Chem* 269: 28777–28782.
109. Tsumoto, K., K. Ogasahara, Y. Ueda, K. Watanabe, K. Yutani, and I. Kumagai. 1995. Role of Tyr residues in the contact region of anti-lysozyme monoclonal antibody HyHEL10 for antigen binding. *J Biol Chem* 270: 18551–18557.
110. Starovasnik, M.A., M.P. O'Connell, W.J. Fairbrother, and R.F. Kelley. 1999. Antibody variable region binding by Staphylococcal protein A: thermodynamic analysis and location of the Fv binding site on E-domain. *Protein Sci* 8: 1423–1431.
111. Yarema, K.J. 2001. New directions in carbohydrate engineering: a metabolic substrate-based approach to modify the cell surface display of sialic acids. *Biotechniques* 31: 384–393.
112. Kuschert, G.S., F. Coulin, C.A. Power, A.E. Proudfoot, R.E. Hubbard, A.J. Hoogewerf, and T.N. Wells. 1999. Glycosaminoglycans interact selectively with chemokines and modulate receptor binding and cellular responses. *Biochemistry* 38: 12959–12968.
113. Fromm, J.R., R.E. Hileman, E.E. Caldwell, J.M. Weiler, and R.J. Linhardt. 1995. Differences in the interaction of heparin with arginine and lysine and the importance of these basic amino acids in the binding of heparin to acidic fibroblast growth factor. *Arch Biochem Biophys* 323: 279–287.

114. Fromm, J.R., R.E. Hileman, E.E. Caldwell, J.M. Weiler, and R.J. Linhardt. 1997. Pattern and spacing of basic amino acids in heparin binding sites. *Arch Biochem Biophys* 343: 92–100.
115. Tyler-Cross, R., M. Sobel, L.E. McAdory, and R.B. Harris. 1996. Structure-function relations of antithrombin III-heparin interactions as assessed by biophysical and biological assays and molecular modeling of peptide-pentasaccharide-docked complexes. *Arch Biochem Biophys* 334: 206–213.
116. Quesenberry, M.S., R.T. Lee, and Y.C. Lee. 1997. Difference in the binding mode of two mannose-binding proteins: demonstration of a selective minicluster effect. *Biochemistry* 36: 2724–2732.
117. Novokhatny, V. and K. Ingham. 1997. Thermodynamics of maltose binding protein unfolding. *Protein Sci* 6: 141–146.
118. Seelig, A., T. Alt, S. Lotz, and G. Holzemann. 1996. Binding of substance P agonists to lipid membranes and to the neurokinin-1 receptor. *Biochemistry* 35: 4365–4374.
119. Wieprecht, T., M. Beyermann, and J. Seelig. 1999. Binding of antibacterial magainin peptides to electrically neutral membranes: thermodynamics and structure. *Biochemistry* 38: 10377–10387.
120. Srivastava, D.K., S. Wang, and K.L. Peterson. 1997. Isothermal titration microcalorimetric studies for the binding of octenoyl-CoA to medium chain acyl-CoA dehydrogenase. *Biochemistry* 36: 6359–6366.
121. Zhang, F. and E.S. Rowe. 1994. Calorimetric studies of the interactions of cytochrome c with dioleoylphosphatidylglycerol extruded vesicles: ionic strength effects. *Biochim Biophys Acta* 1193: 219–225.
122. Simon, S.A. and T.J. McIntosh. 1984. Interdigitated hydrocarbon chain packing causes the biphasic transition behavior in lipid/alcohol suspensions. *Biochim Biophys Acta* 773: 169–172.
123. Anchordoquy, T.J. 1999. Nonviral gene delivery systems, Part 1: Physical stability. *Biopharm* 12: 42–48.
124. Lo, Y.L. and Y.E. Rahman. 1995. Protein location in liposomes, a drug carrier: a prediction by differential scanning calorimetry. *J Pharm Sci* 84: 805–814.
125. Papahajopoulos, D., M. Moscarello, E.H. Eylar, and T. Isac. 1975. Effects of proteins on thermotropic phase transitions of phospholipid membranes. *Biochim Biophys Acta* 401: 317–335.
126. Collins, D. and Y. Cha. 1994. Interaction of recombinant granulocyte colony stimulating factor with lipid membranes: enhanced stability of a water-soluble protein after membrane insertion. *Biochemistry* 33: 4521–4526.
127. Rourke, A.M., Y. Cha, and D. Collins. 1996. Stabilization of granulocyte colony-stimulating factor and structurally analogous growth factors by anionic phospholipids. *Biochemistry* 35: 11913–11917.
128. Maneri, L.R. and P.S. Low. 1989. Fatty acid composition of lipids which copurify with band 3. *Biochem Biophys Res Commun* 159: 1012–1019.
129. Lung-Nan, L., J.F. Brandts, M.J. Brandts, and V.V. Plotnikov. 2002. Determination of the volumetric properties of proteins and other solutes using pressure perturbation calorimetry. *Anal Biochem* 302: 144–160.
130. Helper, L.G. 1969. Thermal expansion and structure in water and aqueous solutions. *Can J Chem* 47: 4613.

131. Palma, R. and P.M. Curmi. 1999. Computational studies on mutant protein stability: the correlation between surface thermal expansion and protein stability. *Protein Sci* 8: 913–920.
132. Joly, M. 1965. *A Physico-Chemical Approach to the Denaturation of Proteins*. Academic Press, London.
133. Lumry, R. and H. Eyring. 1954. Conformation changes of proteins. *J Phys Chem* 58: 110–120.
134. Kauzmann, W. and R.B. Simpson. 1953. Kinetics of protein denaturation. III. Optical rotations of serum albumin, β-lactoglobulin, and pepsin in urea solutions. *J Am Chem* 75: 5154–5157.
135. Tanford, C. 1961. *Physical Chemistry of Macromolecules*. John Wiley & Sons, New York.
136. Remmele, R.L., Jr., J. Zhang, V. Dharmavaram, D. Balaban, M. Durst, A. Shoshitaiskvili, and H. Rand. 2004. Scan-rate dependent melting transitions of interleukin-1 receptor (type II): elucidation of meaningful thermodynamic and kinetic parameters of aggregation acquired from DSC simulations (submitted for publication).
137. Cooper, A., M.A. Nutley, and A. Wadood. 2000. Differential scanning microcalorimetry. In *Protein-Ligand Interactions: Hydrodynamics and Calorimetry.* S.E. Harding and B.Z. Chowdhry, editors. Oxford University Press, Oxford, 287–318.
138. Sanchez-Ruiz, J.M., J.L. Lopez-Lacomba, M. Cortijo, and P.L. Mateo. 1988. Differential scanning calorimetry of the irreversible thermal denaturation of thermolysin. *Biochemistry* 27: 1648–1652.
139. Conejero-Lara, F., J.M. Sanchez-Ruiz, P.L. Mateo, F.J. Burgos, J. Vendrell, and F.X. Aviles. 1991. Differential scanning calorimetric study of carboxypeptidase B, procarboxypeptidase B and its globular activation domain. *Eur J Biochem* 200: 663–670.
140. Privalov, G., V. Kavina, E. Freire, and P.L. Privalov. 1995. Precise scanning calorimeter for studying thermal properties of biological macromolecules in dilute solution. *Anal Biochem* 232: 79–85.
141. Kendrick, B.S., J.F. Carpenter, J.L. Cleland, and T.W. Randolph. 1998. A transient expansion of the native state precedes aggregation of recombinant human interferon-gamma. *Proc Natl Acad Sci U.S.A.* 95: 14142–14146.
142. Su, X.Y., A. Li Wan Po, and S. Yoshioka. 1994. A bayesian approach to Arrhenius prediction of shelf-life. *Pharm Res* 11: 1462–1466.
143. Matsuura, J.E., A.E. Morris, R.R. Ketchem, E.H. Braswell, R. Klinke, W.R. Gombotz, and R.L. Remmele, Jr. 2001. Biophysical characterization of a soluble CD40 ligand (CD154) coiled-coil trimer: evidence of a reversible acid-denatured molten globule. *Arch Biochem Biophys* 392: 208–218.